

Effects of bulk viscosity, heat capacity ratio and Prandtl number on the dispersion relationship of the compressible Navier-Stokes equation

Swagata Bhaumik^{3*}, Sawant Omkar Deepak¹

^{1,2,3}*Department Of Mechanical Engineering, IIT (ISM) Dhanbad, Dhanbad - 826004, India*

Abstract

Here, variation of the dispersion characteristics of 3D linearized compressible Navier-Stokes equation (NSE) with respect to bulk viscosity ratio (κ/μ), specific heat ratio γ and Prandtl number Pr is presented. The 3D compressible NSE supports five type of waves, two vortical, one entropic and two acoustic modes. While the vortical and entropic modes are non-dispersive in nature, the acoustic modes are dispersive only up to a certain bifurcation wavenumber. The characteristics and variation of relative (with respect to the vortical mode) diffusion coefficient for entropic and acoustic modes and a specially designed dispersion function for acoustic modes with depressed wavenumber $\eta = KM/Re$ is presented. We have shown that these functions only depend on η , κ/μ , γ and Prandtl number Pr of the flow. At lower wavenumber components, the deviation of the dispersion function from the inviscid and adiabatic case is proportional to η^2 at the leading order and the relative diffusion coefficients increase linearly with κ/μ and γ while varying inversely with Pr . When the bulk viscosity ratio is increased, the shape and extent of the dispersion function is altered significantly and the change is more significant for higher wavenumber components. The relative diffusion coefficient for entropic and acoustic modes show contrasting variation with wavenumber depending upon κ/μ , γ and Pr . We show by solving linearized compressible NSE that relatively significant evolution and radiation of acoustic and/or entropic disturbances are noted when the bulk viscosity ratio is close to the corresponding critical value for which the bifurcation wavenumber is maximum. Based on this criterion, we have presented a empirical relation to obtain κ/μ depending upon γ and Pr which would indicate the range of bulk viscosity ratio for obtaining relatively significant disturbance evolution.

Key words:

Compressible Navier-Stokes equation, Dispersion relation, Diffusion coefficient, Group velocity, Reynolds number, Mach number, Knudsen number

*Corresponding author

Email address: swagatabhaumik@iitism.ac.in

Email addresses: swagatabhaumik@iitism.ac.in (Swagata Bhaumik³), omkars30.20dr0128@mech.iitism.ac.in (Sawant Omkar Deepak¹)

1. Introduction

Wave mechanics is a fundamental topic in various fields of applied and theoretical physics, like continuum mechanics, electro-magneto-dynamics, quantum mechanics, optics etc. or a combination of these [1, 2]. As described in [2]: “wave is a recognizable signal that is transferred from one part of the medium to another with a recognizable velocity of propagation”. As it propagates, it may undergo distortion, amplitude variation and change in propagation velocity. A definitive class of waves may be classified as dispersive waves for which an analogous dispersion relation relating the wave’s frequency and wavenumber can be derived by incorporating the properties of the medium in which it is propagating. This is a fundamental concept in wave-mechanics and is applicable to various wave phenomena *i.e.*, electromagnetic waves [1], acoustic waves [2], surface gravity and water waves [3] and waves in elastic media [4] and many more. A detailed description of dispersive system may be found in [2, 3, 1].

Here, we attempt to provide a theoretical description of the disturbance evolution characteristics in a compressible, isotropic Newtonian flow by illustrating the variation of its dispersion relation with respect to bulk viscosity ratio, specific heat ratio (γ) and Prandtl number (Pr) from low to high wavenumber range. These studies are important, particularly in the context of the determination of sound radiation and propagation in various gaseous environment. Most of the studies on aeroacoustics have been performed assuming zero-bulk viscosity (Stokes’ hypothesis) [5, 6, 7, 8, 9] and also considering fixed values of γ and Pr . These studies are important and have shed very interesting light on the sources and factors determining far-field acoustic radiation [10, 11]. However, there is a need to augment these by considering real-gas effects which generally has non-zero bulk viscosity[12] but also temperature or density varying γ and Prandtl number Pr (for example in the case of dense or strongly interacting gases). Similar studies by incorporating real-gas effects on radiation characteristics of acoustic/entropic disturbances may be important for high temperature gases (like that inside an internal-combustion engine or over- or under-expanded jets) or in case of different atmospheric conditions (like the planet Jupiter where the atmosphere is predominantly composed of 75% hydrogen and 24% helium or in Mars where the atmosphere is composed of 95% Carbon dioxide). A good review of various recent numerical efforts (mostly 2015 onwards) of simulating high-speed flows involving shocks, turbulence and combustion incorporating bulk viscosity effects is presented in [13] and is not repeated here.

The manuscript is organized as follows: In Sec. 2, a theoretical description of the dispersion relation of the linearized compressible NSE is provided along with governing disturbance evolution equation for vortical, entropic and acoustic modes. The general nature of the dispersion equation and its effect on the dispersive and diffusive behavior of the modes are also illustrated. Section 3 begins with the introduction of relative diffusion coefficients and the dispersion function and subsequently elaborates the variation of these variables with bulk viscosity ratio, specific heat ratio and Prandtl number. The section also presents results for linearized disturbance evolution while varying bulk viscosity ratio for a given initial condition. Additionally, it develops an empirical criterion on the bulk viscosity ratio for which relatively significant

acoustic or entropic disturbance evolution is noted. Lastly, summary and conclusion is presented in Sec. 4.

2. The linearized 3D compressible Navier-Stokes equation

The conservative form of the 3D compressible Navier-Stokes equations (NSE) in vectorial notation are given as

$$\frac{\partial \tilde{\rho}}{\partial t} + \tilde{\nabla} \cdot (\tilde{\rho} \tilde{\mathbf{v}}) = 0 \quad (1)$$

$$\frac{\partial}{\partial t} (\tilde{\rho} \tilde{\mathbf{v}}) + \tilde{\nabla} \cdot (\tilde{\rho} \tilde{\mathbf{v}} \tilde{\mathbf{v}}) = -\tilde{\nabla} \tilde{p} + \tilde{\nabla} \cdot \tilde{\boldsymbol{\tau}} \quad (2)$$

$$\frac{\partial}{\partial t} (\tilde{\rho} \tilde{e}_t) + \tilde{\nabla} \cdot (\tilde{\rho} \tilde{\mathbf{v}} \tilde{h}_t) = \tilde{\nabla} \cdot (\tilde{\boldsymbol{\tau}} \cdot \tilde{\mathbf{v}}) - \tilde{\nabla} \cdot \tilde{\mathbf{q}} \quad (3)$$

Equations (1-3) are written in the dimensional form, where $\tilde{\rho}$ represents fluid density; \tilde{T} represents fluid temperature; \tilde{p} represents thermodynamic pressure; $\tilde{\mathbf{v}}$ represent fluid velocity \tilde{e}_i and $\tilde{e}_t = \frac{1}{2} (\tilde{\mathbf{v}} \cdot \tilde{\mathbf{v}}) + \tilde{e}_i$ represent the specific internal and total energy, respectively; $\tilde{h}_i = \tilde{e}_i + \tilde{p}/\tilde{\rho}$ and $\tilde{h}_t = \tilde{e}_t + \tilde{p}/\tilde{\rho}$ represent specific internal and total enthalpy, respectively; $\tilde{\mathbf{q}}$ represent the heat-flux and $\tilde{\boldsymbol{\tau}}$ represent the components of the viscous stress tensor. For an isotropic and Newtonian fluid obeying Fourier law of heat conduction, the symmetric stress tensor and the heat-flux are given as [14]

$$\tilde{\boldsymbol{\tau}} = -\sigma D \mathbf{I} + 2\mu \tilde{\boldsymbol{\epsilon}}; \quad \tilde{\boldsymbol{\epsilon}} = \frac{1}{2} (\tilde{\nabla} \tilde{\mathbf{v}} + \tilde{\nabla} \tilde{\mathbf{v}}^T) \quad \text{and} \quad \tilde{\mathbf{q}} = -\hat{k} \tilde{\nabla} \tilde{T}$$

Here, $\tilde{\boldsymbol{\epsilon}}$ and $D = \tilde{\nabla} \cdot \tilde{\mathbf{v}}$ is the symmetric strain-rate tensor and the volumetric dilatation rate, respectively. The variables, μ , σ and \hat{k} represent the dynamic and the second coefficient of viscosity and the thermal conductivity of the fluid, respectively. For a Newtonian and isotropic fluid the bulk coefficient of viscosity is obtained $\kappa = (-\sigma + 2\mu/3)$ and according to the Stokes' hypothesis [14] $\sigma = 2\mu/3$ or $\kappa = 0$. For a calorically perfect gas, which is assumed here, the the equation of state is given as $\tilde{p} = R \tilde{\rho} \tilde{T}$ while $\tilde{e}_i = c_v \tilde{T}$ and $\tilde{h}_i = c_p \tilde{T}$. Here, R , $c_v = R/(\gamma - 1)$, $c_p = \gamma R/(\gamma - 1)$ and $\gamma = c_p/c_v$ are the universal gas constant, specific heat at constant volume and constant pressure and ratio of specific heats, respectively.

Next, we consider the evolution of small perturbation by linearizing the Eqs. (1-3) with respect to mean velocity $\mathbf{v}_m = (U_m, V_m, W_m)$, density ρ_m , pressure p_m and temperature T_m . These mean variables are treated here to be truly constant and not functions of space and time. One can non-dimensionalize the resulting linearized equations by using $U = |\mathbf{v}_m| = \sqrt{U_m^2 + V_m^2 + W_m^2}$ as reference velocity scale; ρ_m as reference density scale; T_m as reference temperature scale; $p_m = R\rho_m T_m$ as the reference pressure scale; L as reference length scale and L/U as reference time scale. The resulting non-dimensional perturbation equations are given in the vector notation as

$$\frac{\mathcal{D}\rho'}{\mathcal{D}t} + \nabla \cdot \mathbf{v}' = 0 \quad (4)$$

$$\frac{\mathcal{D}\mathbf{v}'}{\mathcal{D}t} + \frac{1}{\gamma M^2} \nabla p' = \frac{1}{Re} \nabla^2 \mathbf{v}' + \frac{(1-\alpha)}{Re} \nabla (\nabla \cdot \mathbf{v}') \quad (5)$$

$$\frac{\mathcal{D}T'}{\mathcal{D}t} + (\gamma - 1) \nabla \cdot \mathbf{v}' = \frac{\gamma}{Pr} \frac{1}{Re} \nabla^2 T' \quad (6)$$

where $\alpha = \sigma/\mu = (2/3 - \kappa/\mu)$ and $Re = \mu/\rho_m UL$, $Pr = c_p \mu/\hat{k}$ and $M = U/\sqrt{\gamma RT_m}$ is the Reynolds number, Prandtl number and the Mach number of the mean-flow, respectively. In Eqs. (4-6), the operator $\mathcal{D}/\mathcal{D}t$ is defined as $\mathcal{D}/\mathcal{D}t = (\partial/\partial t + \mathbf{c} \cdot \nabla)$, where $\mathbf{c} = (c_x, c_y, c_z)$ such that $c_x = U_m/U$, $c_y = V_m/U$ and $c_z = W_m/U$.

One can also relate the disturbance pressure p' , density ρ' and temperature T' using the non-dimensional perturbed equation of state which for an ideal calorically perfect gas is given as

$$p' = (\rho' + T') \quad (7)$$

The non-dimensional perturbation entropy s' and vorticity $\boldsymbol{\Omega}'$ are given as $s' = T' - p'(\gamma - 1)/\gamma$ and $\boldsymbol{\Omega}' = \nabla \times \mathbf{v}'$, respectively. Therefore, the evolution equation for s' and $\boldsymbol{\Omega}'$ are given as

$$\frac{\mathcal{D}s'}{\mathcal{D}t} = \frac{1}{Pr} \frac{1}{Re} \nabla^2 T' \quad (8)$$

$$\frac{\mathcal{D}\boldsymbol{\Omega}'}{\mathcal{D}t} = \frac{1}{Re} \nabla^2 \boldsymbol{\Omega}' \quad (9)$$

Hence, the linearized vorticity transport equation is essentially given by the 3D convection-diffusion equation. One notes that because of the linearization of the governing equations, nonlinear baroclinic source term are absent in Eq. (9).

2.1. Physical dispersion relation of 3D-LNSE

We obtain the physical dispersion relation of 3D-LNSE given by Eqs. (4-6) by denoting the physical variables in terms of corresponding Fourier-Laplace amplitudes as

$$(\rho', \mathbf{v}', T')^T = \int \int \int \left(\hat{\xi}, \hat{\Phi}, \hat{\theta} \right)^T e^{i(k_x x + k_y y + k_z z - \omega t)} dk_x dk_y dk_z \quad (10)$$

where, k_x , k_y and k_z are wavenumbers along x -, y - and z -directions, respectively, while ω represents the complex frequency and $i = \sqrt{-1}$. Note that $\omega = \omega_R + i\omega_I$ is a complex quantity such that ω_R denotes the real frequency while ω_I denotes the temporal growth rate of the disturbances. On substituting Eq. (10) in Eqs. (4-6), the evolution eigenvalue equation is obtained as $[\mathbf{D} - i\omega\mathbf{I}] \left(\hat{\xi}, \hat{\Phi}, \hat{\theta} \right)^T = 0$. Hence, the physical dispersion relation is obtained by setting

$$|\mathbf{D} - i\omega\mathbf{I}| = \begin{vmatrix} \Lambda & ik_x & ik_y & ik_z & 0 \\ \frac{1}{\gamma M^2} ik_x & \Lambda + \Delta_1 & \Delta_5 & \Delta_6 & \frac{1}{\gamma M^2} ik_x \\ \frac{1}{\gamma M^2} ik_y & \Delta_5 & \Lambda + \Delta_2 & \Delta_7 & \frac{1}{\gamma M^2} ik_y \\ \frac{1}{\gamma M^2} ik_z & \Delta_6 & \Delta_7 & \Lambda + \Delta_3 & \frac{1}{\gamma M^2} ik_z \\ 0 & (\gamma - 1) ik_x & (\gamma - 1) ik_y & (\gamma - 1) ik_z & \Lambda + \Delta_4 \end{vmatrix} = 0 \quad (11)$$

where $\Lambda = i(\beta - \omega)$, $\beta = k_x c_x + k_y c_y + k_z c_z = \mathbf{K} \cdot \mathbf{c}$, $\mathbf{K} = (k_x, k_y, k_z)$, $\Delta_1 = ((2 - \alpha)k_x^2 + k_y^2 + k_z^2)/Re$, $\Delta_2 = (k_x^2 + (2 - \alpha)k_y^2 + k_z^2)/Re$, $\Delta_3 = (k_x^2 + k_y^2 + (2 - \alpha)k_z^2)/Re$, $\Delta_4 = \gamma(k_x^2 + k_y^2 + k_z^2)/(RePr)$, $\Delta_5 = (1 - \alpha)k_x k_y/Re$, $\Delta_6 = (1 - \alpha)k_x k_z/Re$ and $\Delta_7 = (1 - \alpha)k_y k_z/Re$. Here, $\mathbf{K} = (k_x, k_y, k_z)$ denotes the wavenumber vector whose modulus is given as $K = \sqrt{k_x^2 + k_y^2 + k_z^2}$.

Simplifying the above relation, the characteristic equation is obtained as

$$\Lambda^5 + C_1 z_1 \Lambda^4 + (C_2 z_1^2 + z_2) \Lambda^3 + (C_3 z_1 z_2 + C_4 z_1^3) \Lambda^2 + (C_5 z_1^4 + C_6 z_1^2 z_2) \Lambda + C_7 z_1^3 z_2 = 0 \quad (12)$$

where, $z_1 = K^2/Re$, $z_2 = (K/M)^2$, $K = \sqrt{k_x^2 + k_y^2 + k_z^2}$, $C_1 = (4 - \alpha) + \gamma/Pr$, $C_2 = (5 - 2\alpha) + (4 - \alpha)\gamma/Pr$, $C_3 = (2 + 1/Pr)$, $C_4 = (2 - \alpha) + (5 - 2\alpha)\gamma/Pr$, $C_5 = (2 - \alpha)\gamma/Pr$, $C_6 = (1 + 2/Pr)$, and $C_7 = 1/Pr$. It may be noted that defining the depressed absolute wavenumber $\eta = \sqrt{z_1^2/z_2} = (KM/Re)$ and scaled dispersion variable $\lambda = \Lambda/z_1$, Eq. (12) may be expressed in terms of λ as

$$\lambda^5 + C_1 \lambda^4 + \left(C_2 + \frac{1}{\eta^2}\right) \lambda^3 + \left(\frac{C_3}{\eta^2} + C_4\right) \lambda^2 + \left(C_5 + \frac{C_6}{\eta^2}\right) \lambda + \frac{C_7}{\eta^2} = 0 \quad (13)$$

Equation (12) is a quintic polynomial equation and generally solutions of any polynomial equation of degree five or higher can not be expressed in terms of radicals of the coefficients according to Abel-Ruffini theorem [15]. However, this is not applicable here. One notes that the dispersion relationship can be expressed as $\omega_j = \beta + i\Lambda_j = \beta + iz_1 \lambda_j$ where $j = 1, 2, 3, 4, 5$ and segregating the real and imaginary parts, $\omega_{jR} = \beta - \Lambda_{jI}$ and $\omega_{jI} = \Lambda_{jR}$. It may be noted that the nondimensional number M/Re appearing the expression for η , defines the ratio of the sound propagation time to the momentum diffusivity time [16]. This number may also be related to the Knudsen number $Kn = l/L$, where l is the mean-free path of the fluid molecules. Following classical Maxwell-Boltzmann theory of a mono-atomic gas $M/Re = Kn\sqrt{2/(\pi\gamma)}$ [17].

The $3D-LNSE$ is in general dispersive and diffusive in nature. For the inviscid and adiabatic (and hence isentropic) case which corresponds to the linearized Euler equation (LEE), $C_1 = C_2 = C_3 = C_4 = C_5 = C_6 = C_7 = 0$ and therefore, $\omega_{1,2,3} = \beta$ while $\omega_{4,5} = \beta \mp K/M$. Therefore, the modes corresponding to $\omega_{1,2,3}$ are non-dispersive and non-dissipative which only convects with the flow. As for the LEE, $\mathcal{D}\Omega'/\mathcal{D}t = \mathcal{D}s'/\mathcal{D}t = 0$ and therefore, $\omega_{1,2,3}$ represent two vortical and one entropic modes, respectively. The modes denoted by $\omega_{4,5}$ are dispersive and non-diffusive. The propagation speed of these modes depends on the Mach number M of the mean flow. These modes represent the two acoustic modes. This can be justified by considering the fact that following LEE, the acoustic equation corresponding to p' is given as

$$\left(\frac{\mathcal{D}}{\mathcal{D}t}\right)^2 p' - \frac{1}{M^2} \nabla^2 p' = 0 \quad (14)$$

for which the dispersion relation is also given by $\omega = \beta \mp K/M$. For the present viscous case, p' may be considered to be caused by acoustic and entropic disturbances simultaneously. Hence, using Eqs. (4) and (5) and the relationship $p' = \gamma(\rho' + s')$ that the modified acoustic relation may be obtained as

$$\left(\frac{\mathcal{D}}{\mathcal{D}t}\right)^2 \rho' - \left(\frac{2 - \alpha}{Re}\right) \left(\frac{\mathcal{D}}{\mathcal{D}t}\right) \nabla^2 \rho' - \frac{1}{M^2} \nabla^2 \rho' = \frac{1}{M^2} \nabla^2 s' \quad (15)$$

Therefore, for the viscous case, the entropic perturbations act as a source term to the acoustic wave propagation which are dissipative and dispersive in nature. In all subsequent discussions, modes-1 and 2 represent two vortical modes; mode-3 represents the entropic mode and modes-4 and 5 represent the acoustic mode-1 and 2, respectively.

It can be shown from the characteristic Eq. (12) that $\Lambda_{1,2} = -z_1 = -K^2/Re$ are two roots of Eq. (12) and the associated dispersion relation is given as $\omega_{1,2} = \beta - iK^2/Re$. These two modes correspond to the vortical mode as can be readily noted from the perturbation linearized vorticity transport Eq. (9). Factoring out these two roots from Eq. (12), the dispersion relation for one entropic and the two acoustic modes are given by the following cubic equation

$$\Lambda^3 + C_8 z_1 \Lambda^2 + (C_5 z_1^2 + z_2) \Lambda + C_7 z_1 z_2 = 0 \quad (16)$$

where $C_8 = (2 - \alpha) + \gamma/Pr$. In terms of $\lambda = \Lambda/z_1$, Eq. (16) may be expressed as

$$\lambda^3 + C_8 \lambda^2 + (C_5 + 1/\eta^2) \lambda + C_7/\eta^2 = 0 \quad (17)$$

It may be noted that for any general cubic equation, the roots may be obtained by applying the Cardano's method followed by Vieta's substitution [18]. Similar dispersion analysis are also given in [19] for 1D-linearized compressible NSE. For 1D compressible NSE, considering heat-transfer one has only the entropic and the two acoustic modes and hence the dispersion relation is also given by a cubic equation [19].

One notes that all the coefficients of Eq. (16) are real, indicating that it has either one real root (Λ_3) and two complex conjugate roots (Λ_4 and Λ_5) or three real roots. The real Λ_3 represents the entropic while the complex conjugate Λ_4 and Λ_5 denotes the acoustic modes. The analytical solution of a cubic polynomial equation is explained in Appendix-I for the ease of the reader.

2.2. Group velocity, phase velocity and diffusion coefficient

For the above dispersive system, one can define the physical group velocity and the phase-speed of the j^{th} -mode along x -direction as[2]

$$V_{gx}^j = \frac{\partial \omega_{jR}}{\partial k_x} = c_x - \frac{d\Lambda_{jI}}{dK} \frac{k_x}{K} \quad (18)$$

$$c_{px}^j = \frac{\omega_{jR}}{k_x} \quad (19)$$

The group velocity and the phase speed along y - and z -directions can also be similarly defined. For a system with complex ω , the physical wave solution grows in time as $e^{\omega t}$. This can be used to define the diffusion coefficient of the j^{th} -mode as

$$\nu_j = -\frac{\omega_{jI}}{K^2} = -\frac{\Lambda_{jR}}{K^2} \quad (20)$$

The rationale behind such a definition stems from the behavior of the solution of the multi-dimensional linear advection-diffusion equation $\frac{\partial f}{\partial t} + \mathbf{c} \cdot \nabla f = \nu \nabla^2 f$, for which the complex dispersion relation is given as $\omega = \beta - i\nu K^2$ and the solution of the corresponding Cauchy problem decays with time as $e^{-\nu K^2 t}$.

One notes that for the vortical mode $V_{gx}^{(1,2)} = c_x$, $V_{gy}^{(1,2)} = c_y$, $V_{gz}^{(1,2)} = c_z$ and $\nu_{(1,2)} = 1/Re$. Hence, the vortical modes are non-dispersive but diffusive in nature and the diffusion coefficient does not depend on the wavenumber. As Λ_3 is also a real root of Eq. (16), the entropic mode is also non-dispersive and diffusive in nature, like the vortical modes. Therefore, $V_{gx}^3 = c_x$, $V_{gy}^3 = c_y$ and $V_{gz}^3 = c_z$. However, unlike the vortical mode, the diffusion coefficient ν_3 for the entropic mode depends on the wavenumber as well as all the other parameters, *viz.*, flow Mach number M , the Reynolds number Re , bulk viscosity ratio κ/μ , ratio of the specific heats γ and the Prandtl number Pr . The acoustic modes are also diffusive in nature, while these can be dispersive or non-dispersive depending upon the wavenumber. This aspect is illustrated next.

2.3. Estimation of the bifurcation wavenumber

From Eq. (16) which is a cubic equation with real coefficients, one notes that two scenarios may arise depending upon whether (a) it has one real and two complex conjugate roots or (b) three real roots. For case-(a), $\Lambda_{4R} = \Lambda_{5R}$ (and hence, $\nu_4 = \nu_5$) and $\Lambda_{4I} = -\Lambda_{5I}$. For this case, the two acoustic modes have identical diffusion coefficient while these propagate in opposite directions relative to the mean flow. For case-(b), $\Lambda_{4R} \neq \Lambda_{5R}$ in general (indicating $\nu_4 \neq \nu_5$) and $\Lambda_{4I} = \Lambda_{5I} = 0$. Hence for case-(b), two acoustic modes have different diffusion coefficient while these are non-dispersive in nature. The bifurcation wavenumber K_b between cases-(a) and (b) can be obtained by setting the discriminant Δ of the cubic dispersion Eq. (16) to zero. If $\Delta > 0$, we have case-(a) while for $\Delta < 0$, we have case-(b). It may be noted that for any general cubic equation with real coefficients, $ax^3 + bx^2 + cx + d = 0$, the expression for the discriminant is given as $\Delta = (b^2c^2 - 4ac^3 - 4b^3d - 27a^2d^2 + 18abcd)$ [18]. For Eq. (16), setting associated $\Delta = 0$, one gets the following cubic equation for the depressed bifurcation wavenumber $\eta_b = (K_b M/Re)$ as

$$C_9 z_b^3 + C_{10} z_b^2 + C_{11} z_b - 4 = 0 \quad (21)$$

where, $z_b = \eta_b^2$, $C_9 = (C_8^2 C_5^2 - 4C_5^3)$, $C_{10} = (2C_5 C_8^2 - 12C_5^2 - 4C_8^3 C_7 + 18C_5 C_7 C_8)$, $C_{11} = (C_8^2 - 12C_5 - 27C_7^2 + 18C_7 C_8)$. The physical value of η_b is obtained from the real positive root of Eq. (21). It is to be noted that the coefficients C_9 , C_{10} and C_{11} are polynomial functions of the parameters $g = (2 - \alpha) = (4/3 + \kappa/\mu)$, $\xi_1 = \gamma/Pr$ and $\xi_2 = 1/Pr$. In fact, these coefficients are given as $C_9 = g^2 \xi_1^2 (g - \xi_1)^2$, $C_{10} = 2g \xi_1 (g + \xi_1)^2 - 12g^2 \xi_1^2 - 4\xi_2 (g + \xi_1)^3 + 18g \xi_1 \xi_2 (g + \xi_1)$ and $C_{11} = (g + \xi_1)^2 + 18\xi_2 (g + \xi_1) - 27\xi_2^2 - 12g \xi_1$.

3. Results and Discussion

Here, we illustrate the dispersive and the diffusive characteristics of the modes. Firstly, we define relative diffusion coefficient $\nu_j/\nu_1 = \lambda_{jR}/\lambda_{1R}$ and dispersion function $\widehat{\mathcal{M}}_j = \lambda_{jI}\eta^2 = \Lambda_{jI}(M^2/Re)$. We illustrate results by mostly plotting these variables as a function of the depressed absolute wavenumber $\eta = (KM/Re)$. We chose η , instead of the absolute wavenumber K as the independent variable, as it makes the variables ν_j/ν_1 and $\widehat{\mathcal{M}}_j$ independent of the Mach number M and the Reynolds number Re of the flow. These variables

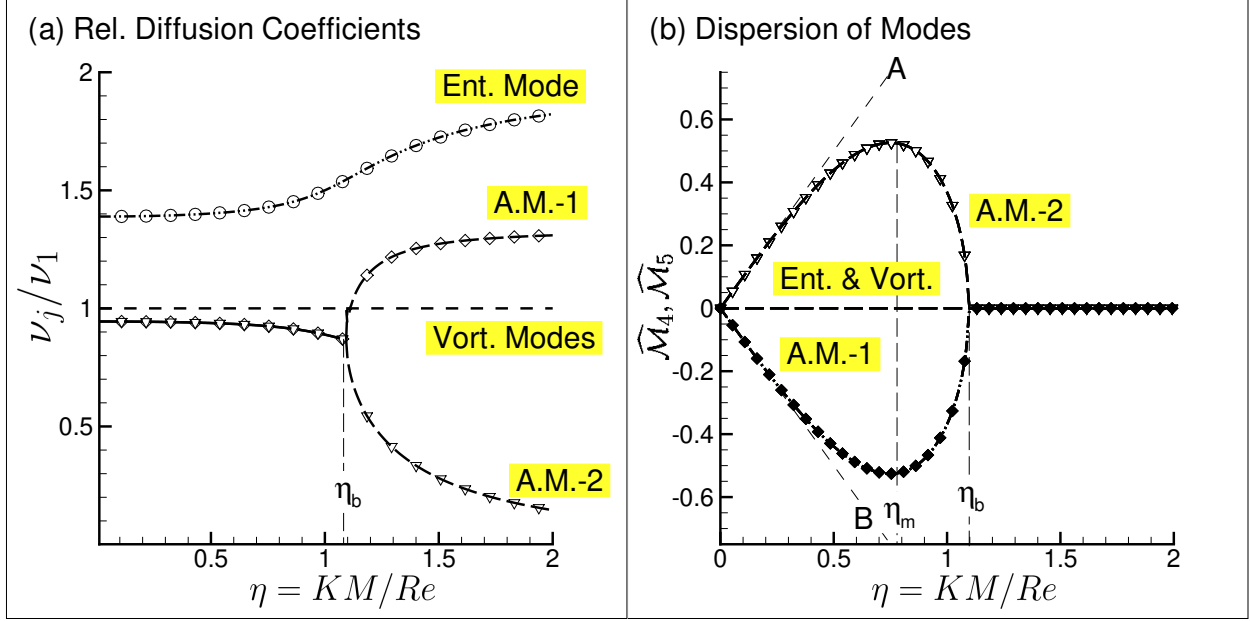


Figure 1: (a) ν_j/ν_1 and (b) $\widehat{\mathcal{M}}_{4,5}$ plotted as a function of the depressed absolute wavenumber $\eta = KM/Re$ for $\kappa/\mu = 0$, $\gamma = 1.4$ and $Pr = 0.72$. The two straight-lines A and B represents $\widehat{\mathcal{M}}_{4,5} = \mp\eta$, respectively.

when expressed as a function of η only depends upon the parameters α (or κ/μ), γ and the Prandtl number Pr of the flow. For the inviscid and adiabatic flows (which are governed by the LEE), $\Lambda_{(1,2,3)} = 0$ and $\Lambda_{(4,5)} = \mp i(K/M)$. Therefore, $\widehat{\mathcal{M}}_{(1,2,3)} = 0$ and $\widehat{\mathcal{M}}_{(4,5)} = \mp\eta$ for such cases.

3.1. General dispersive and the diffusive characteristics of the modes

In Fig. 1(a) and 1(b), we plot ν_j/ν_1 and $\widehat{\mathcal{M}}_{4,5}$ as a function of η for $\kappa/\mu = 0$, $\gamma = 1.4$ and $Pr = 0.72$, respectively. The values corresponding to γ and Pr correspond to the values for a standard atmosphere while $\kappa/\mu = 0$ following the Stokes' hypothesis[14]. Figure 1(a) shows that the entropic mode is more diffusive than the vortical mode and the two acoustic modes. The acoustic modes are less diffusive than the vortical mode up to $\eta = \eta_b$. The depressed bifurcation wavenumber η_b corresponds to the situation when the discriminant of the dispersion relation Eq. (17) becomes zero as noted in Sec. 2.3. For $\eta < \eta_b$ both the acoustic modes have identical diffusion while these display opposite dispersion characteristics. At $\eta = \eta_b$, a bifurcation in the diffusion coefficient for acoustic modes occurs as noted in Fig. 1(a). For $\eta > \eta_b$, while the diffusion coefficient for the acoustic mode-1 increases and is more than the vortical mode at high-wavenumbers, that for the acoustic mode-2 decreases. Figure 1(b) shows that $\widehat{\mathcal{M}}_{(1,2,3)} = 0$, indicating that entropic and the vortical modes are non-dispersive in nature. For the acoustic modes $\widehat{\mathcal{M}}_4 = -\widehat{\mathcal{M}}_5$ for $\eta < \eta_b$, indicating that acoustic modes-1 and 2 propagates along opposite directions relative to the mean flow. The two straight-lines A and B in Fig. 1(b) represents $\widehat{\mathcal{M}} = \pm\eta$, respectively which indicates the dispersion relation for the upstream and the downstream (relative to the mean flow) propagating acoustic modes for the inviscid

and adiabatic case. For $\eta < \eta_c \approx 0.4$, we note $|\widehat{\mathcal{M}}_{(4,5)}| \approx \eta$. Therefore, dispersion (not diffusion) of large wavelength disturbances can still be estimated by LEE. This aspect is illustrated later in Sec. 3.2. The dispersion function $\widehat{\mathcal{M}}_{(4,5)}$ is dominated by viscous actions for $0.4 \lesssim \eta \leq \eta_b$. At $\eta = \eta_m \approx 0.7\eta_b$ a local minima or maxima is noted to form for the dispersion function $\widehat{\mathcal{M}}_{4,5}$ corresponding to the acoustic mode-1 and -2, respectively. Beyond $\eta > \eta_b$, $\widehat{\mathcal{M}}_{(4,5)} = 0$, indicating that the acoustic modes are non-dispersive in nature.

Here, we may draw the parallel of the dispersion relationship with the Grad's moment system derived by projecting the Boltzmann equation using physically realizable distribution function. The obtained equations describe the macroscopic governing equations for locally conserved density, momentum and energy, the non-equilibrium stress tensor and energy flux vector etc. and is considered a benchmark for the subsequent theoretical developments in the area of non-equilibrium thermodynamics [20]. The dispersion relation of the 1D linearized Grad's moment system is considered in Refs. [21] and [22]. The obtained dispersion relation bears a strong resemblance with the current one derived from linearized compressible NSE.

3.2. Asymptotic solution of the dispersion equation for $\eta < 1$

When $\eta < 1$, generally $\eta < \eta_b$ and the discriminant of Eq. (16) $\Delta > 0$. Therefore, the acoustic modes are dispersive in nature indicating λ_3 is purely real and $\lambda_{4,5}$ are complex conjugates. For the cubic equation given by Eq. (17) the analytical solution is illustrated in Appendix-I. For the case with $\Delta > 0$, the solutions for $\lambda_{3,4,5}$ are given as in the form shown through Eqs. (39). The expression for the discriminant is given in Eq. (37). Also see Eq. (43) where Δ is expressed in terms of η . From these equations, one can express $\lambda_{3,4,5}$ as

$$\lambda_3 = \frac{1}{3} \left(\frac{4}{3} + \frac{\kappa}{\mu} + \frac{\gamma}{Pr} \right) + u_1 \quad (22)$$

$$\lambda_{4,5} = \left[\frac{1}{3} \left(\frac{4}{3} + \frac{\kappa}{\mu} + \frac{\gamma}{Pr} \right) - \frac{1}{2} u_1 \right] \pm i \frac{\sqrt{3}}{2} v_1 \quad (23)$$

The expressions for u_1 and v_1 are given in Sec. 5.2. For $\eta \ll 1$, one can expand $\sqrt{\Delta}$ and subsequently $\sqrt[3]{R_1}$ and $\sqrt[3]{R_2}$ in terms of η and thereby obtains the following expressions for u_1 and v_1 as $u_1 = (e_1 + e_3\eta^2 + e_5\eta^4 + \dots)$ and $v_1 = [2/(\sqrt{3}\eta)] (1 + e_2\eta^2 + e_4\eta^4 + e_6\eta^6 + \dots)$. Putting these in Eq. (23) and noting $z_1/\eta = K/M$, one obtains the dispersion relation for the entropic and the acoustic modes when $\eta < 1$ as

$$\omega_3 = \beta - iz_1 \left[\frac{1}{3} \left(\frac{4}{3} + \frac{\kappa}{\mu} + \frac{\gamma}{Pr} \right) + (e_1 + e_3\eta^2 + e_5\eta^4 + \dots) \right] \quad (24)$$

$$\omega_{4,5} = \left\{ \beta \mp \frac{K}{M} (1 + e_2\eta^2 + e_4\eta^4 + e_6\eta^6 + \dots) \right\} - iz_1 \left[\frac{1}{3} \left(\frac{4}{3} + \frac{\kappa}{\mu} + \frac{\gamma}{Pr} \right) - \frac{1}{2} (e_1 + e_3\eta^2 + e_5\eta^4 + \dots) \right] \quad (25)$$

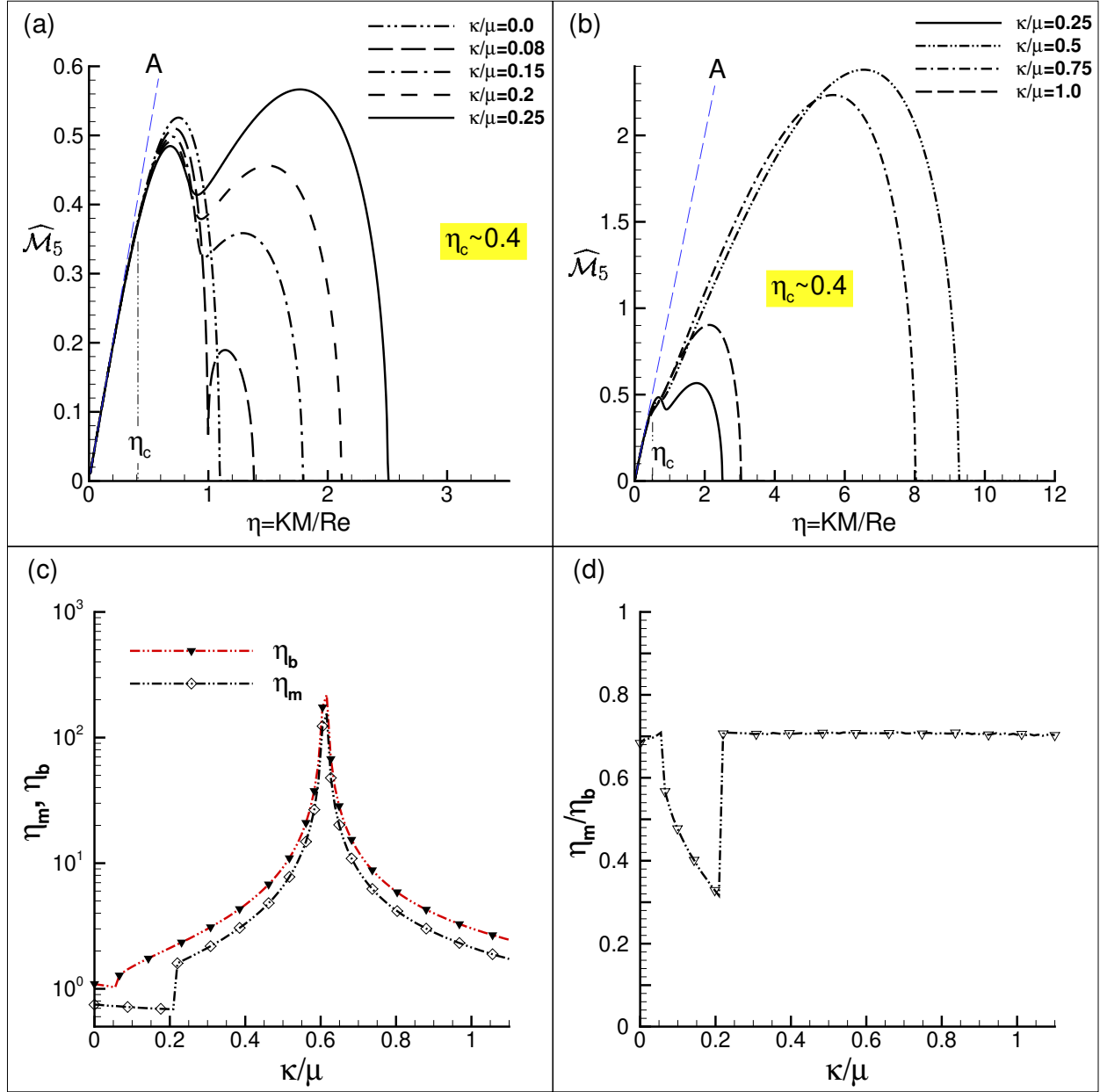


Figure 2: (a,b) The dispersion function $\widehat{\mathcal{M}}_5$ for acoustic mode-2 plotted as a function of $\eta = KM/Re$ for indicated values of κ/μ when $\gamma = 1.4$ and $Pr = 0.72$. (c,d) η_b , η_m and η_b/η_m plotted as a function of κ/μ , respectively.

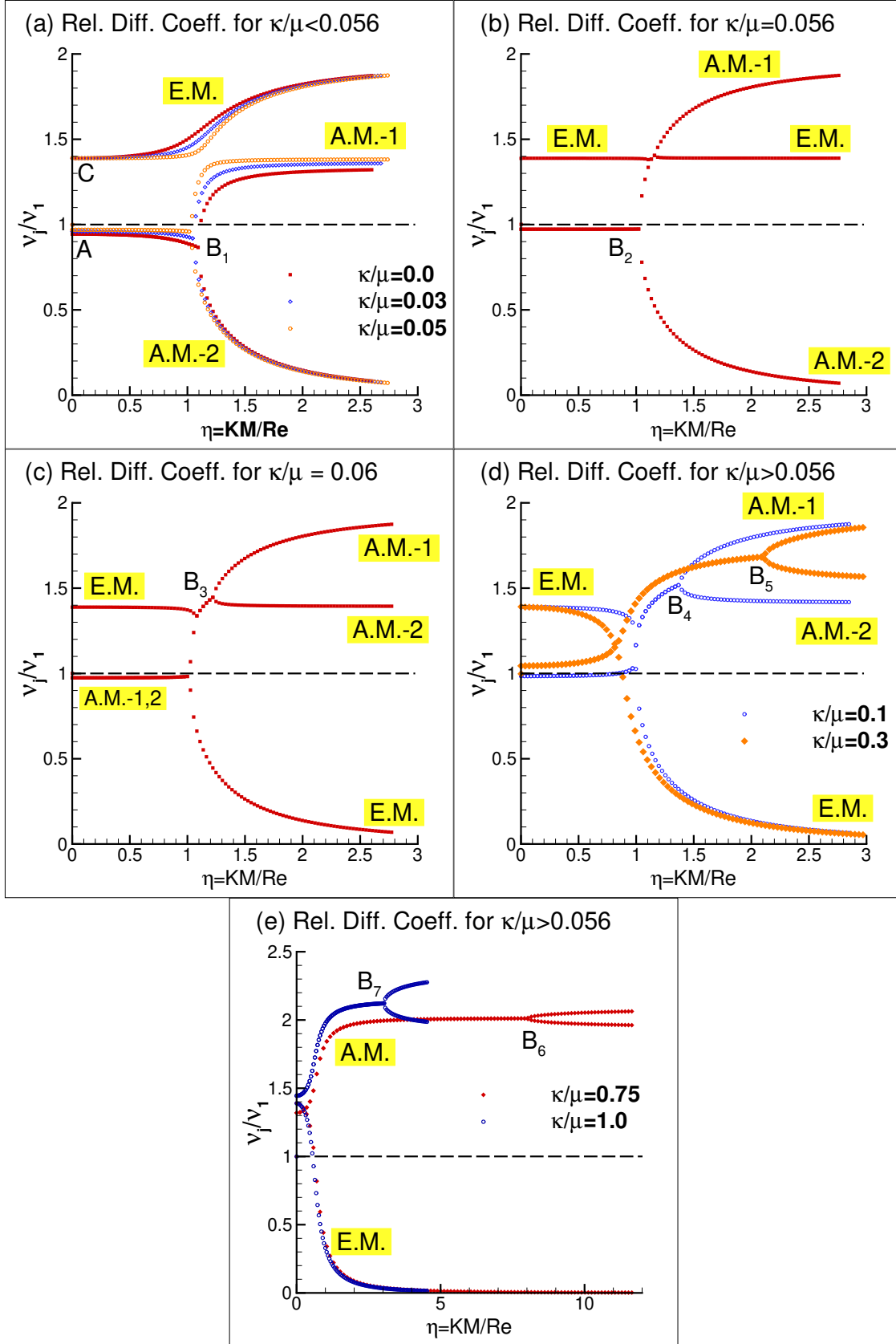


Figure 3: v_j/v_1 for entropic and acoustic modes plotted as a function of $\eta = KM/Re$ for indicated values of κ/μ when $\gamma = 1.4$ and $Pr = 0.72$. The bifurcation points are marked with B_k where $k = 1, \dots, 7$.

Therefore, the entropic mode is non-dispersive in nature, whereas for the acoustic modes one gets back the dispersion relation $\omega_{4,5} = \beta \mp K/M$ for inviscid and adiabatic case. One also notes that for $\eta < 1$, the relative diffusion coefficients for the entropic and acoustic modes from Eq. (25) are given as

$$\frac{\nu_3}{\nu_1} = \left[\frac{1}{3} \left(\frac{4}{3} + \frac{\kappa}{\mu} + \frac{\gamma}{Pr} \right) + (e_1 + e_3\eta^2 + e_5\eta^4 + \dots) \right] \quad (26)$$

$$\frac{\nu_{4,5}}{\nu_1} = \left[\frac{1}{3} \left(\frac{4}{3} + \frac{\kappa}{\mu} + \frac{\gamma}{Pr} \right) - \frac{1}{2} (e_1 + e_3\eta^2 + e_5\eta^4 + \dots) \right] \quad (27)$$

The coefficients e_1, \dots, e_5 are functions of $b_0, b_1, d_0, \dots, d_3$. The last coefficients are given in Sec. 5.4 in terms of $\kappa/\mu, \gamma/Pr$ and $1/Pr$. The coefficients e_1, \dots, e_5 as functions of $b_0, b_1, d_0 \dots d_3$ are given as

$$\begin{aligned} e_1 &= \left(\frac{2}{27} b_1 \right); \quad e_2 = \left(\frac{9}{2} d_2 - \frac{1}{243} b_1^2 \right); \quad e_3 = 2 \left(\frac{729}{19683} b_0 - \frac{6561}{19683} b_1 d_2 + \frac{5}{19683} b_1^3 \right); \\ e_4 &= \left(\frac{9}{2} d_1 - \frac{2}{243} b_0 b_1 + \frac{5}{54} b_1^2 d_2 - \frac{10}{177147} b_1^4 - \frac{405}{8} d_2^2 \right); \\ e_5 &= -2 \left(\frac{1}{3} b_0 d_2 + \frac{1}{3} b_1 d_1 - \frac{5}{6561} b_0 b_1^2 - 6 b_1 d_2^2 + \frac{20}{2187} b_1^3 d_2 - \frac{22}{4782969} b_1^5 \right); \\ e_6 &= \left(\frac{9}{2} d_0 - \frac{405}{4} d_1 d_2 - \frac{40}{177147} b_0 b_1^3 + \frac{5}{54} b_1^2 d_1 + \frac{55}{19683} b_1^4 d_2 - \frac{1}{243} b_0^2 - \frac{154}{129140163} b_1^6 \right. \\ &\quad \left. + \frac{13365}{16} d_2^3 - \frac{55}{24} b_1^2 d_2^2 + \frac{5}{27} b_0 b_1 d_2 \right) \end{aligned}$$

Therefore, in the long wavelength limit ($\eta \ll 1$), the relative diffusion coefficients of the entropic and acoustic modes increase linearly with κ/μ and γ while these variations are inversely proportional to Pr .

3.3. Effect of bulk viscosity ratio κ/μ on dispersion characteristics

There are several recent efforts in determining the bulk viscosity of the fluid and its effects on the flow under various conditions. In [13], Green-Kubo method is used to study the bulk viscosity of several dilute gases and their mixtures. Similar efforts are also performed in [23],[24],[25] to determine κ for various gases using molecular dynamics simulations. The bulk viscosity ratio κ/μ have been estimated to range from a very small number to 4 for Argon [25], 0.01 – 2 for gaseous CO₂[25], from 0.5 – 0.7 for N₂ [13], from 0.5 – 0.6 for O₂ and similar values for N₂-O₂ mixture[13] and from 0.6 – 1.75 for dry air [13, 24, 26] depending upon density and temperature.

In Figs. 2(a,b), we plot the dispersion function $\widehat{\mathcal{M}}_5$ as a function of η for indicated κ/μ cases with $\gamma = 1.4$ and $Pr = 0.72$. As noted in Fig. 1(b), $\widehat{\mathcal{M}}_5$ for $\kappa/\mu = 0$, initially monotonically increases, reaches maxima at $\eta = \eta_m$ and subsequently decreases to zero at $\eta = \eta_b$. With increase in κ/μ from 0 to 0.25, a secondary peak is noted to gradually arise. For all these cases, however, $\widehat{\mathcal{M}}_5 \approx \eta$ for $\eta \lesssim 0.4$. This indicates that change in bulk viscosity in this regime has less significant effect on the dispersion function for the spectral components having wavenumbers smaller than $\eta \lesssim 0.4$, and these follow the inviscid isentropic dispersion function given by LEE. This may be noted by comparing the deviation of $\widehat{\mathcal{M}}_5$ with the line *A* which depicts the variation of the dispersion function from LEE. A detailed analysis in the low wavenumber regime is provided in the previous subsection.

The increase in κ/μ from 0 to 0.25 is noted to significantly alter the dispersion relation of higher wavenumber components firstly due to the appearance of a secondary peak, whose extent is noted to grow from $\kappa/\mu = 0.08$ to 0.25 and secondly due to increase in η_b . For $\kappa/\mu = 0.25$, we note the secondary peak to be more dominant than the primary one. As the bulk viscosity ratio is further increased from 0.25 we note the initial primary one to merge with the secondary one and thereby loses its distinct signature. The previous secondary peak becomes the sole dominant one for $\kappa/\mu \gtrsim 0.3$. One also notes from Fig. 2(b) that η_b to first increase, reaches a maximum value and subsequently decrease with increase in κ/μ .

The last aspect is further explored in Fig. 2(c) where, η_b and η_m is plotted as a function of κ/μ . One notes from this figure that η_b to be maximum at $\kappa/\mu \simeq 0.6$. The corresponding value of η_b at $\kappa/\mu \approx 0.6$ is roughly two orders of magnitude higher than that at $\kappa/\mu = 0$. The value of η_m corresponding to the peak location for the dispersion function $\widehat{\mathcal{M}}_5$ remains virtually constant up to $\kappa/\mu \simeq 0.2$, at which point a discontinuous change is noted. This is related with almost unchanged location of the primary peak, appearance of a secondary peak and the eventual dominance of the latter beyond $\kappa/\mu \gtrsim 0.2$. It may be noted that beyond $\kappa/\mu \simeq 0.2$, the η_m follows similar trend as that shown by η_b . In fact, for $\kappa/\mu \gtrsim 0.2$, η_m/η_b remains almost constant at 0.7 as shown in Fig. 2(d).

3.4. Effect of bulk viscosity ratio κ/μ on diffusion characteristics

Next, we illustrate the variation of the relative diffusion coefficient ν_j/ν_1 for the entropic and the acoustic modes when κ/μ is varied for $\gamma = 1.4$ and $Pr = 0.72$. This is shown in Fig. 3 where the abbreviations *E.M.*, *A.M. - 1* and *A.M. - 2* denote the entropic, acoustic modes-1 and -2, respectively. We note three different trends depending upon whether κ/μ is less than, equal to or more than 0.56. The first trend is noted when $\kappa/\mu < 0.56$. some typical cases are shown in Fig. 3(a). For this case, following observations may be noted:

1. The entropic mode is more diffusive than the vortical mode while ν_3/ν_1 increases with increase in η as the coefficient e_3 in Eq. (27) is positive.
2. The acoustic modes are less diffusive and $\nu_{(4,5)}/\nu_1$ is noted to decrease with increase in η for $\eta < \eta_b$ as $e_3 > 0$. The bifurcation point η_b is marked as B_1 in Fig. 3(b).
3. For $\eta > \eta_b$, while the relative diffusion coefficient of the acoustic mode-1 is intermediate between the vortical and the entropic modes, it monotonically decrease for the acoustic mode-2 with increase in η .

In all subsequent discussions, we denote similar trend for the variation of the relative diffusion coefficients as T_1 for easy reference. For the cases shown in Fig. 3(a), we also note that with increase in κ/μ , ν_3/ν_1 decreases and tends to become more flatter. Similarly, the level of ν_5/ν_1 increases with increase in κ/μ beyond $\eta = \eta_b$ and likewise tend to become flatter for high η components.

At $\kappa/\mu = 0.56$, the ν_3/ν_1 becomes independent of η , which is formed by connecting the increasingly flatter parts of the entropic and the acoustic mode-2 beyond the bifurcation wavenumber as noted in Fig. 3(b). The relative diffusion coefficients of the acoustic modes are also noted to be independent of η up to the bifurcation point B_2 . Such a variation is noted probably because all the coefficients e_3, e_5, \dots become vanishingly small

for this combination of parameters. Such a trend of variation is denoted hereafter as T_0 for easy reference. Trend T_0 indicates that the entropic and acoustic modes are essentially decoupled and the entropic mode effectively follows a convection-diffusion equation.

Beyond $\kappa/\mu > 0.56$, altered variation of the relative diffusion coefficients are noted which become more prominent as κ/μ increases further. For these cases, while ν_3/ν_1 monotonically decreases, the $\nu_{(4,5)}/\nu_1$ for $\eta < \eta_b$ monotonically increases with η . Not only these variation become steeper but also a gradual increase in the level of relative diffusion coefficients for the acoustic modes before the bifurcation point occurs with increase in κ/μ . Similar trends are subsequently referred to as T_2 . We later see these trends are generic and also noted when γ or Pr is parametrically varied.

3.5. Linearized disturbance evolution

To assess the implication of the above analysis on the effects of bulk viscosity ratio, we perform the linearized evolution of disturbances by varying bulk viscosity ratio κ/μ . We specifically perform the initial value problem, where the initial condition in the form of a wave-packet containing multiple spectral components is imposed as a combination of entropic and acoustic disturbances. Solution of similar test problem was also reported in [27]. The exact solution of the linearized *NSE* given by Eqs. (4-6) may be obtained by considering the Fourier transform as given by Eq. (10). The evolution equation of the Fourier amplitudes are given as

$$\frac{\partial}{\partial t} \{\mathcal{F}\} + [D] \{\mathcal{F}\} = 0 \quad (28)$$

where, $\{\mathcal{F}\} = (\xi, \hat{\Phi}, \theta)^T$ and the matrix $[D]$ indicates the corresponding evolution matrix. From Eq. (28), one obtains the exact solution for $\mathcal{F}(t)$ considering a periodic problem as

$$\{\mathcal{F}\} = [R] e^{\{-\chi\}t} [L] \{\mathcal{F}_0\} \quad (29)$$

where $\{\mathcal{F}_0\}$ is the Fourier amplitudes corresponding to the initial perturbations, while $[R]$, $[L]$ and $[\chi]$ are the right-eigenvector, left-eigenvector and eigenvalue matrices corresponding to $[D]$ such that $[D] = [R][\chi][L]$. Therefor, diagonal entries of $[\chi]$ are given as $\chi_j = i\omega_j = i\beta - \Lambda_j$, so that Λ_j are the roots of the dispersion equation given by Eq. (12). The right-eigenvector appearing in Eq. (28) for a 3D-problem may be symbolically given as

$$[R] = \begin{bmatrix} r_1 & r_2 & r_3 \\ 0 & 0 & 1 \\ \mathbf{K} \times \delta_1/K & \mathbf{K} \times \delta_2/K & -i\mathbf{K}F_j/z_1M^2 \\ 0 & 0 & (\gamma - 1)H_j \end{bmatrix} \quad (30)$$

where $j = 3, 4, 5$; $\delta_1 = (0, 0, 1)^T$; $\delta_2 = (0, 1, 0)^T$; $F_j = \gamma(\lambda_j + 1/Pr) / [(\lambda_j + (2 - \alpha))(\lambda_j + \gamma/Pr)]$; $H_j = \lambda_j / (\lambda_j + \gamma/Pr)$ and λ_j are the roots of the characteristic Eq. (17) for entropic and acoustic modes. Here, the column vectors r_1, r_2, r_3, r_4 and r_5 represents eigenvectors corresponding to two vortical, entropic, acoustic mode-1 and -2, respectively. One notes that while the perturbation velocity components corresponding to

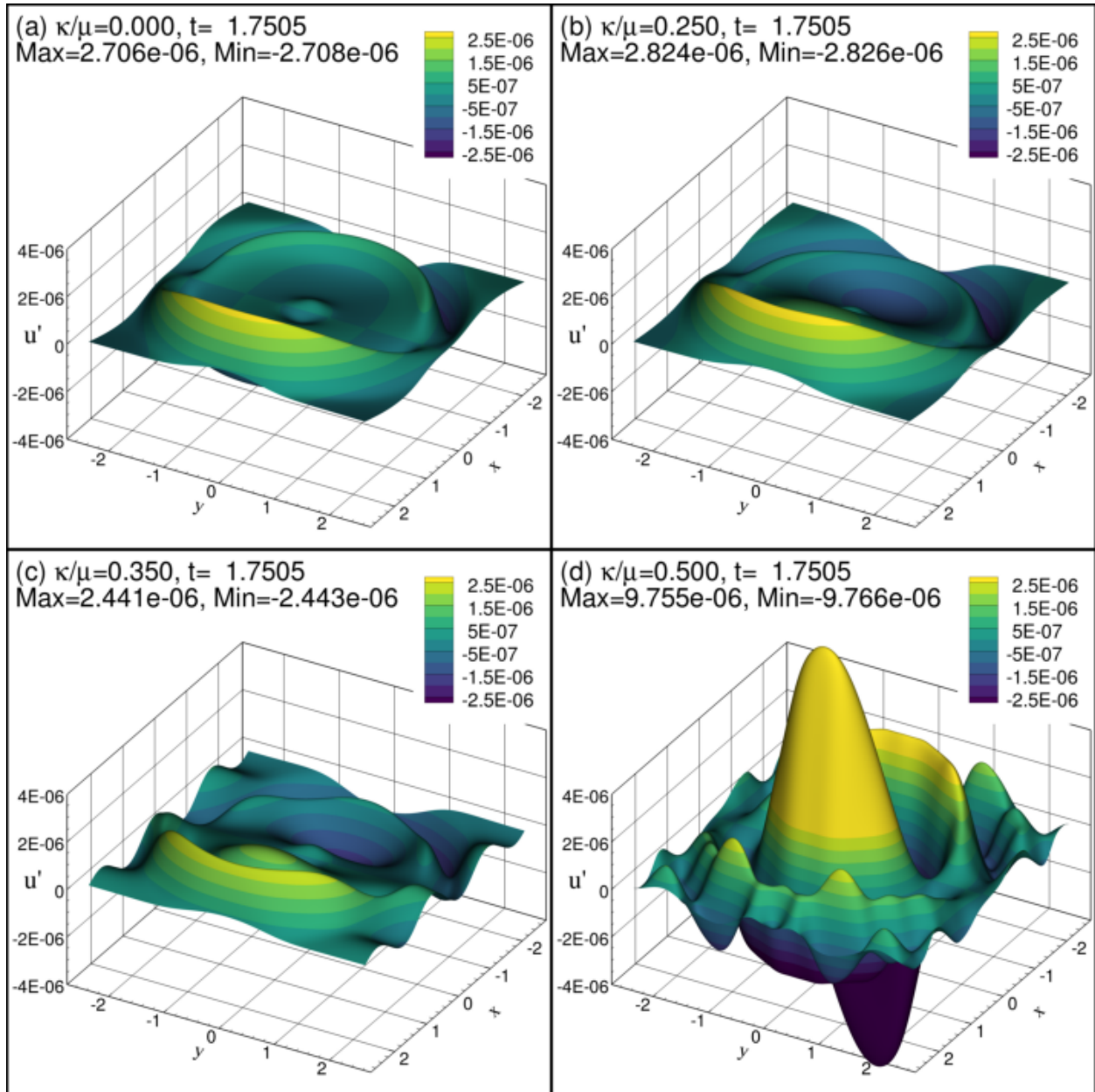


Figure 4: Disturbance u -velocity plotted in the (x, y) -plane at $t = 1.75$ for indicated values of κ/μ . Here, $M = 0.8$, $Re = 100$, $\gamma = 1.4$ and $Pr = 0.72$.

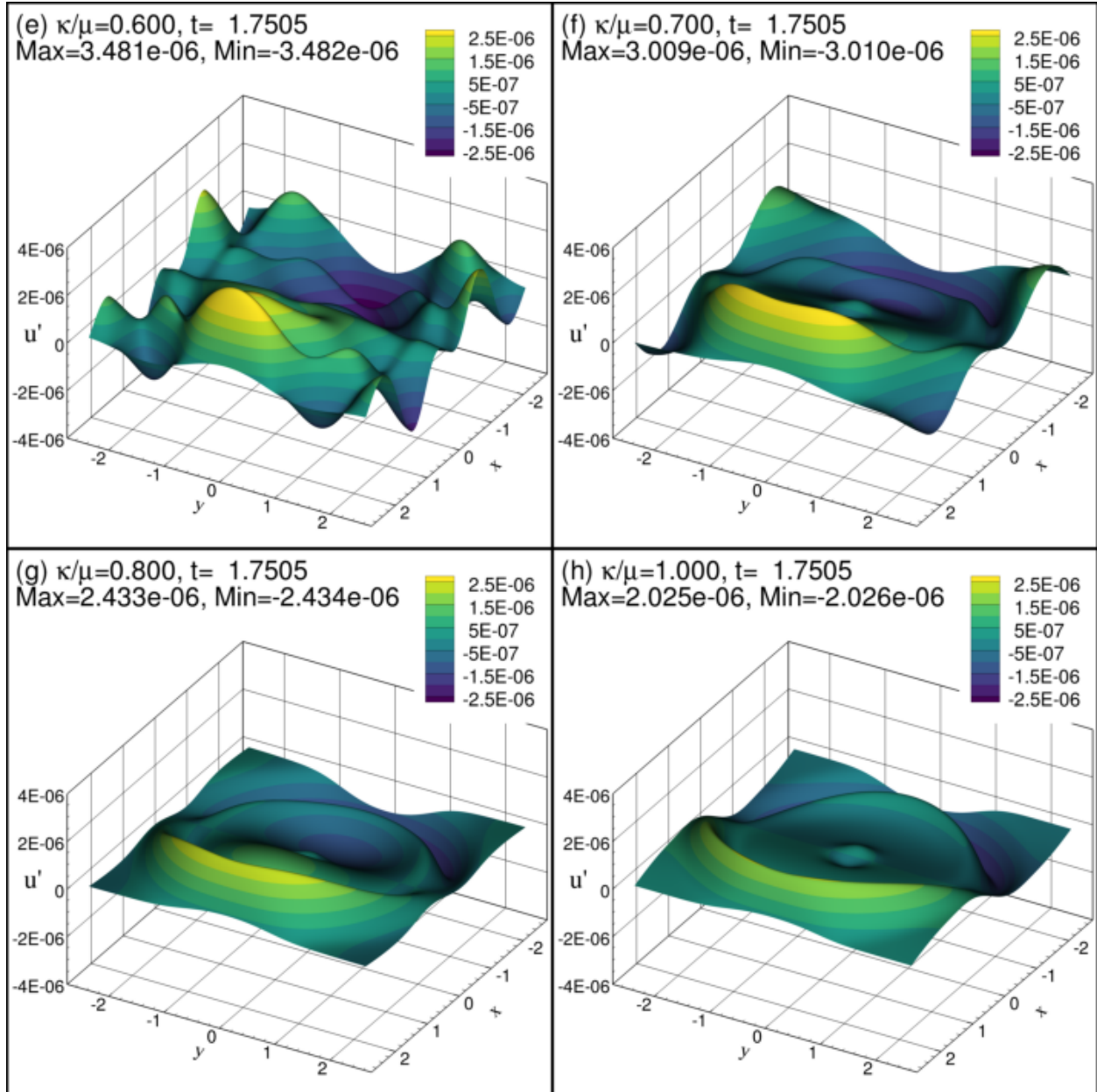


Figure 5: Disturbance u -velocity plotted in the (x, y) -plane at $t = 1.75$ for indicated values of κ/μ . Here, $M = 0.8$, $Re = 100$, $\gamma = 1.4$ and $Pr = 0.72$.

the vortical eigenvectors are solenoidal, those corresponding to entropic and acoustic modes are irrotational. This follows the theoretical criterion postulated in [28] to identify the entropic and acoustic modes.

For the ease of computation, here we consider only the a $2D$ -problem. It may be noted that $2D$ compressible NSE supports four waves, one vortical, one entropic and two acoustic waves. The dispersion relation of the entropic and two acoustic waves for a $2D$ problem is still given by Eq. (16) or Eq. (17), only difference being that here the wavenumber vector $\mathbf{K} = (k_x, k_y)$ and therefore, $K = \sqrt{k_x^2 + k_y^2}$. The right eigenvector described in Eq. (30) is slightly modified for the $2D$ -problem which supports only one vortical mode. The spectral nature of entropic and acoustic modes with respect to the absolute wavenumber remain identical. Once $\mathcal{F}(t)$ is obtained following Eq. (29), the original perturbation quantities can be computed by performing inverse Fourier transform. In actual computation, we first perform fast Fourier transform (FFT) of the initial perturbation, time advance \mathcal{F} using Eq. (29) and obtain back the exact solution at the intended time instant by performing inverse FFT (IFFT).

The physical domain extends from -2.5 to 2.5 along each directions and we used a total of 501 uniformly distributed points to represent the physical domain with a grid spacing of $\Delta x = \Delta y = 0.01$. The results are reported for $M = 0.8$, $Re = 100$, $\gamma = 1.4$ and $Pr = 0.72$ while the mean flow is directed at an angle of $\theta = \tan^{-1}(c_y/c_x) = 45^\circ$. We impose the initial disturbance as

$$\begin{aligned}
p'(x, y, 0) &= p_a(x, y) \\
\rho'(x, y, 0) &= \frac{1}{\gamma} p_a(x, y) - \theta_e(x, y) \\
T'(x, y, 0) &= \left(\frac{\gamma - 1}{\gamma} \right) p_a(x, y) + \theta_e(x, y) \\
p_a(x, y) = \theta_e(x, y) &= \left(\sum_{m,n} \cos [k_{0x_m} (x - x_0) + \varphi_{x_m}] \cos [k_{0y_n} (y - y_0) + \varphi_{y_n}] \right) e^{(-\sigma r^2)} \\
u'(x, y, 0) &= v'(x, y, 0) = 0
\end{aligned} \tag{31}$$

where $r = \sqrt{(x - x_0)^2 + (y - y_0)^2}$ while p_a and θ_e indicate initial disturbances corresponding to acoustic and the entropic pulse, respectively. The center of the pulse is initially located at the position $(x_0, y_0) = (0.25, 0.25)$. Here, k_{0x_m} and φ_{x_m} are the central wavenumber of the wave-packet and the phase, respectively along the x -direction for the m^{th} -mode. We use a total of $m = 101$ and $n = 101$ discrete wavenumbers along x - and y -directions, respectively, such that $k_{0x_m} \Delta x$ and $k_{0y_n} \Delta y$ each spans from 0.1 to 2.0. For any discrete computation, maximum allowable resolution is limited by the Nyquist limit such that $k_{0x_{max}} \Delta x = k_{0y_{max}} \Delta y = \pi$. The phase φ_{x_m} and φ_{y_n} is specified such that it varies randomly between 0 and 2π with uniform probability distribution. We note that the depressed wavenumber η for the initial imposed disturbances spans from $\eta_{min} = 0.08$ to $\eta_{max} = 1.6$. Here, the initial perturbation entropy $s'(x, y, 0) = \theta_e$ and vorticity $\Omega'(x, y, 0) = 0$.

Figures 4 and 5 shows the disturbance u -velocity component at $t = 1.75$ for indicated values of κ/μ . We have also noted the maximum and minimum values of the disturbance in these frames for a specific value of

κ/μ . In Fig. 4(a), when $\kappa/\mu = 0$, one notes two peripheral lobes with a dip at the center. As one increases κ/μ , the intensity of the wavy disturbances are noted to increase. At $\kappa/\mu = 0.5$, we note significantly higher amount of disturbance as compared to $\kappa/\mu = 0, 0.25$ and 0.3 . Further increase in κ/μ gradually brings the disturbance to the level of $\kappa/\mu = 0$, *i.e.*, the case with zero bulk viscosity. The topology of the u' -surface for higher κ/μ cases ($\kappa/\mu = 0.75$ and 1.0) are similar to the lower κ/μ cases ($\kappa/\mu = 0.0$ and 0.25). The results indicate that effects of the bulk viscosity ratio is significant when $\kappa/\mu \simeq 0.5$ where relatively significant disturbance level is noted. For this bulk viscosity ratio the relative diffusion coefficients are less and the extent of dispersive wavenumbers are large. Similar results are also noted when only acoustic disturbances are imposed as the initial condition (results not reported here). We note that according to Fig. 2(c), $(\eta_b)_{max}$ is noted for $\kappa/\mu \simeq 0.6$ which is close to the bulk viscosity ratio for which relatively significant disturbance evolution is observed here. Here lies the importance of Fig. 2(c) which specifies the range of κ/μ that would yield significant acoustic and entropic disturbance evolution, radiation and dispersion. This range of κ/μ may be identified by those, that are close to the one for which η_b is maximum. Moreover, as dispersion may enhance the process of energy cascade in the presence of nonlinearities [29], these range of κ/μ is expected to play a crucial role in the generation of fine-scale turbulence along with playing an important role in acoustic radiation. These aspects may be investigated by direct numerical simulation (DNS) of a system with bulk viscosity ratios laying in these range.

3.6. Physical estimation of the minimum wavelength for the dispersive waves

It is imperative to give a physical explanation of the depressed wavenumber $\eta = KM/Re$. Expressing $M = U_m/c$ and $Re = \rho_m U_m L / \mu_m$, where $c = \sqrt{\gamma RT_m}$ is the speed of sound, one obtains $\eta = (2\pi/\lambda^*)(\mu_m/\rho_m c)$. Here, λ^* is the dimensional wavelength of the disturbances. For an estimate, consider air at standard atmospheric pressure ($101 KPa$) and temperature of 20° . At these standard atmospheric conditions, the density ρ_m , coefficient of dynamic viscosity μ_m and speed of sound c are approximately $\rho_m \simeq 1.225 Kg/m^3$, $\mu_m \simeq 1.81 \times 10^{-5} Pa.s$ and $c \simeq 330 m/s$. Therefore, the ratio $(\mu_m/\rho_m c)$ comes out to be $4.48 \times 10^{-8} m$. Hence, considering $\eta_b \approx \mathcal{O}(1)$, the smallest wavelength of dispersive acoustic disturbances is roughly $\lambda_{min}^* \approx 2.81 \times 10^{-7} m$ whereas, at standard atmospheric conditions the mean free path of the air molecules is roughly $l = 66 nm$ [30]. Therefore, for this case λ_{min}^* is one order of magnitude higher than l and high-wavenumber acoustic dispersive disturbances as predicted by NSE are at the boundaries of the continuum hypothesis [31, 32]. When the bulk viscosity ratio κ/μ is in the range of $0.4 - 0.6$, λ_{min}^* becomes of the same order as l . These scales are, however, smaller than Kolmogorov length-scale $\bar{\eta}_k = Re^{-3/4} l_0$ which defines the length-scales associated with locally isotropic smallest eddies in a highly turbulent flow, where l_0 is the integral length scale [33]. For a turbulent flow with $Re \simeq 10^6$, Kolmogorov length-scale $\bar{\eta}_k \simeq 3.2 \times 10^{-5} m$. In Table 1 we tabulate the properties of some common gases like Carbon dioxide (CO_2), Oxygen (O_2), Carbon monoxide (CO), Hydrogen (H_2), Nitrogen (N_2), dry air and Argon (Ar) at atmospheric pressure and $T = 300K$ and $900K$. We provide a column for λ_{min}^* assuming $\eta_b = 1$. One notes that λ_{min}^* is almost 5 times more than l for most of the gases.

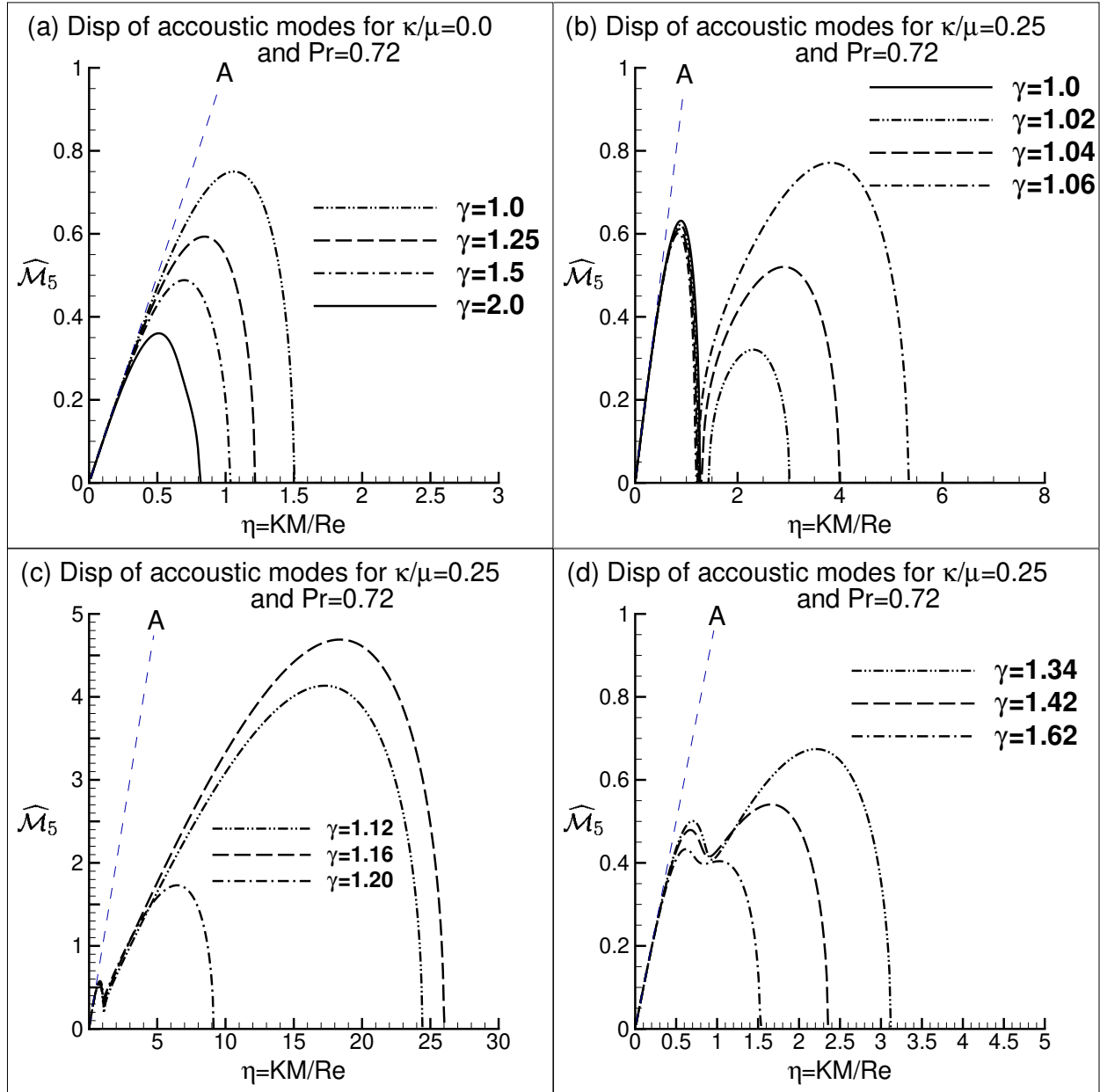


Figure 6: The dispersion function $\widehat{\mathcal{M}}_5$ for the acoustic mode-2 plotted as a function of $\eta = KM/Re$ for indicated values of $\gamma = 1.4$ when (a) $\kappa/\mu = 0.0$ and (b,c,d) $\kappa/\mu = 0.25$. Here, and $Pr = 0.72$. The straight-line A represents $\widehat{\mathcal{M}}_5 = \eta$, *i.e.*, the dispersion function for the inviscid and adiabatic case.

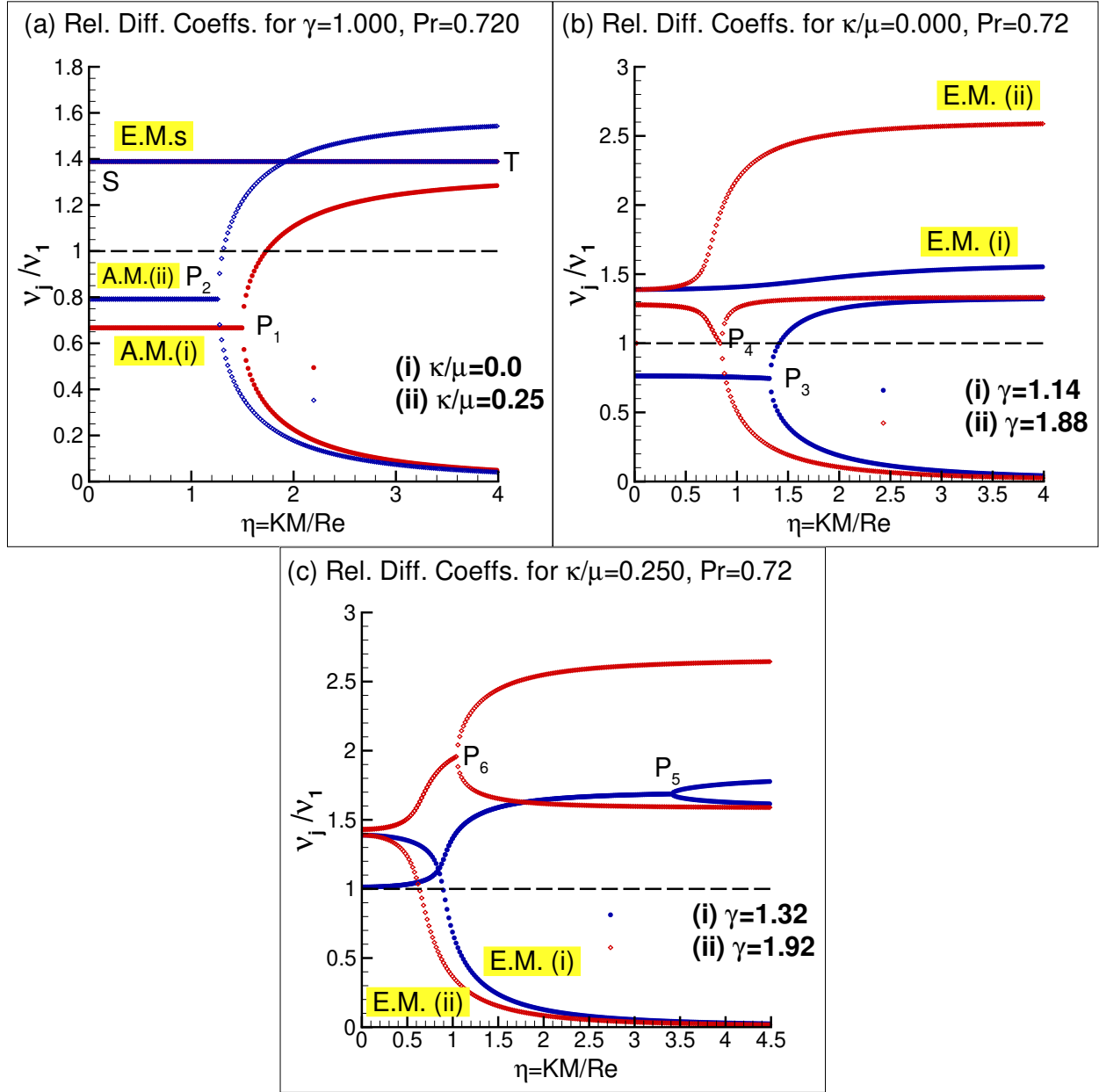


Figure 7: ν_j/ν_1 for entropic and acoustic modes plotted as a function of $\eta = KM/Re$ for indicated values of γ and κ/μ when $Pr = 0.72$. The bifurcation points are marked with P_k where $k = 1, \dots, 5$.

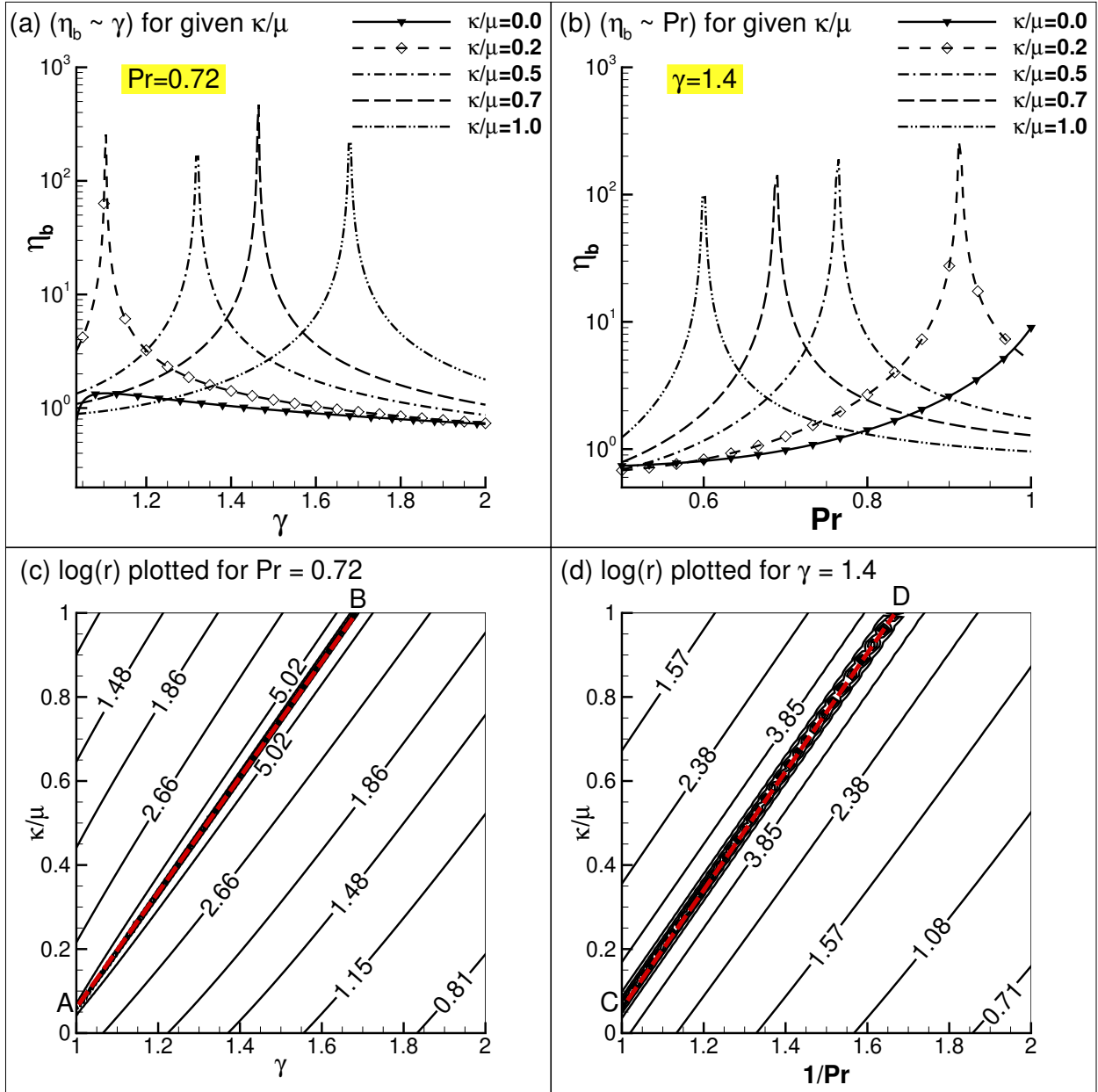


Figure 8: (a,b) η_b plotted as a function of γ and Pr for indicated values of κ/μ , respectively. (c,d) $\log(\hat{r})$ for the cubic Eq. (21) corresponding to η_b^2 shown plotted in $(\kappa/\mu, \gamma)$ and $(\kappa/\mu, 1/Pr)$ -planes for indicated values of Pr and γ , respectively. Here, \hat{r} is the radius of the circle in the complex plane on which the three real solutions of any cubic Eq. (21) lie for negative discriminant (See Eq. (38) in Appendix-I).

Name of the Gas	T (K)	ρ (Kg/m^3)	γ	c (m/s)	μ ($Pa.s$)	\hat{k} ($Watt/K.m$)	Pr	l (m)	λ_{min}^* (m)
CO ₂	300	1.796	1.293	268.31	1.49×10^{-5}	0.0166	0.769	8.45×10^{-8}	1.95×10^{-7}
	900	0.596	1.186	447.18	3.61×10^{-5}	–	–	2.53×10^{-7}	8.52×10^{-7}
O ₂	300	1.301	1.396	329.62	2.06×10^{-5}	0.0268	0.709	7.69×10^{-8}	3.02×10^{-7}
	900	0.433	1.319	555.66	4.45×10^{-5}	–	–	2.31×10^{-7}	1.16×10^{-6}
CO	300	1.138	1.401	353.10	1.79×10^{-5}	0.0252	0.737	6.51×10^{-8}	2.79×10^{-7}
	900	0.379	1.343	599.06	3.89×10^{-5}	–	–	1.95×10^{-7}	1.08×10^{-6}
H ₂	300	0.082	1.405	1319.11	8.96×10^{-6}	0.1817	0.706	1.1×10^{-7}	5.21×10^{-7}
N ₂	300	1.138	1.401	353.13	1.79×10^{-5}	0.0261	0.714	6.94×10^{-8}	2.79×10^{-7}
	900	0.379	1.35	600.8	3.75×10^{-5}	0.0603	0.712	2.08×10^{-7}	1.03×10^{-6}
Dry Air	300	1.177	1.4017	347.33	1.85×10^{-5}	0.0262	0.708	6.66×10^{-8}	2.84×10^{-7}
	900	0.392	1.345	589.65	3.9×10^{-5}	0.0628	0.696	1.73×10^{-7}	1.06×10^{-6}
Ar	300	1.624	1.67	322.66	2.29×10^{-5}	0.0177	0.677	7.96×10^{-8}	2.75×10^{-7}
	900	0.541	1.667	559.11	5.06×10^{-5}	0.0398	0.661	2.39×10^{-7}	1.05×10^{-6}

Table 1: Properties of some common gases at atmospheric pressure and $T = 300K$ and $900K$. All the variables are in *SI* units. The data for density ρ , specific heat ratio γ , speed of sound c , dynamic viscosity μ , thermal conductivity \hat{k} and Prandtl number Pr are taken from [34]. The mean free path is calculated assuming classical Maxwell-Boltzmann theory as $l = k_B T / (\sqrt{2} \pi d^2 P)$ [17], where k_B is the Boltzmann constant and d is the effective diameter of the molecule. Also, $\lambda_{min}^* = 2\pi\mu / (\rho c)$ is the minimum wavelength of the dispersive acoustic disturbances assuming $\eta_b = 1$.

3.7. Effects of specific heat ratio γ and Prandtl number Pr on the dispersion relation

Apart from the bulk viscosity ratio, two other important parameters in the dispersion relation is the specific heat ratio γ and the Prandtl number $Pr = c_p \mu / \hat{k}$. As $\gamma = c_p / c_v$, $\gamma \geq 1.0$ following the second law of thermodynamics [14]. For gases with mono-atomic molecules, the classical Maxwell-Boltzmann distribution specifies $\gamma = 5/3$, whereas for the gases with diatomic or polyatomic molecules, these values theoretically are given as $7/5$ and $4/3$, respectively considering the molecules as rigid particles connected by massless links [17]. Similarly, the classical equipartition of energy predicts that γ is related to the thermally accessible degrees of freedom (f) as $\gamma = 1 + 1/f$ [17]. For common gases like CO₂, O₂, CO, H₂, N₂, air, Argon etc., the value of γ is noted to decrease with temperature [31] (only Argon displays very marginal increase at high temperature). For these gases, the value of γ varies between $1.41 - 1.17$, $1.42 - 1.19$, $1.43 - 1.28$, $1.65 - 1.3$, $1.42 - 1.19$, $1.42 - 1.19$ and $1.70 - 1.65$, respectively when temperature is varied from very low to very high[31]. Also, refer to Table 1 for typical values of γ for some common gases at standard atmospheric pressure and two temperatures of $300K$ and $900K$.

Here, we investigate the specific heat ratio by varying it from $\gamma = 1.0$ to 2.0 . For $\gamma = 1.0$, Eq. (17) may be solved analytically and the corresponding solutions are given as

$$\lambda_3 = -\frac{1}{Pr} \quad \text{and} \quad \lambda_{4,5} = -\alpha_* \pm \sqrt{\alpha_*^2 - \frac{1}{\eta^2}} \quad (32)$$

where $\alpha_* = (2/3 + \kappa/(2\mu))$. Therefore, $\nu_3/\nu_1 = 1/Pr$ and is independent of the depressed wavenumber.

Similarly, before the bifurcation point, the relative diffusion coefficients of the acoustic modes are also constant at $\nu_{4,5}/\nu_1 = \alpha_*$ while $\eta_b = 1/\alpha_*$. Following Eq. (6), we note that for $\gamma = 1$, the entropic mode follows a convection-diffusion equation (for $\gamma = 1$, $s' = T'$).

In Fig. 6, we show the dispersion function $\widehat{\mathcal{M}}_5$ for the acoustic modes as a function of $\eta = KM/Re$ for indicated values of $\gamma = 1.4$. While the variation corresponding to $\kappa/\mu = 0.0$ is shown in frame (a), frames (b,c,d) are for $\kappa/\mu = 0.25$. For all the plots Prandtl number is fixed at 0.72. From Fig. 6(a), we note that the dispersive zone keeps shrinking with increase in γ for $\kappa/\mu = 0$, consequently, the range of wavenumber zone for which one can apply the dispersion relation for the inviscid and the adiabatic case (from LEE) also decrease with increase in γ . For $\kappa/\mu = 0.25$, the trend of the dispersion function is similar to what is noted in Fig. 2(a,b) when the bulk viscosity ratio was varied. When γ is close but slightly more than one, we note the existence of two dispersive zones (see the curve for $\gamma = 1.02$ in Fig. 6(b)). Subsequent increase in γ increases η_b as well as the extent of the zone where deviation from inviscid and adiabatic dispersion function is noted. Beyond $\gamma = 1.16$, the extent of the dispersive zone starts shrinking as shown in Fig. 6(d). This situation is similar to the case when only κ/μ was varied alone (shown in Fig. 2(b)). For the case with $\kappa/\mu = 0.25$, the range of η for which the dispersion function may be approximated by that obtained from LEE remains almost invariant with change in the value of γ . For higher values of κ/μ , the trend remains similar to as noted for $\kappa/\mu = 0.25$, with the value of γ corresponding to $(\eta_b)_{max}$ increasing. This feature would be illustrated later in Fig. 8.

In Fig. 7, we show the variation of the relative diffusion coefficient with depressed wavenumber η when γ is varied. When $\gamma = 1.0$, the relative diffusion coefficient ν_3/ν_1 for $\kappa/\mu = 0$ and 0.25 is identical and invariant of η as also predicted by Eq. (32). Similarly, $\nu_{(4,5)}/\nu_1$ is constant in the dispersive zone before the corresponding bifurcation point η_b . The value of this constant relative diffusion coefficient is given by the corresponding value for α_* for $\kappa/\mu = 0$ and 0.25, respectively. So, it follows the trend T_0 as described in Sec. 3.4. As γ is increased the variation of relative diffusion coefficients show different trends for $\kappa/\mu = 0$ and 0.25 as shown in Fig. 7(b,c). For the first case trend T_1 is followed which is shown in Fig. 7(b) for $\kappa/\mu = 0$ and $\gamma > 1$. Here, ν_3/ν_1 monotonically increase with η while being more than 1 and $\nu_{(4,5)}/\nu_1$ monotonically decreases for $\eta < \eta_b$. For $\kappa/\mu = 0.25$ and $\gamma > 1$, trend T_2 is observed as shown in Fig. 7(c). Here, ν_3/ν_1 monotonically decreases while that for the acoustic modes increase for $\eta < \eta_b$. For both the cases, the level of relative diffusion coefficient increases as γ is increased. For even higher values of κ/μ , the trend for the relative diffusion coefficients is similar to T_2 .

Another factor appearing in the dispersion relationship is the Prandtl number $Pr = c_p\mu/\hat{k}$ which is a ratio of momentum and thermal diffusivity [31, 35]. Typical values of Pr for common gases are tabulated in Table 1. For common gases, Pr is slightly less than 1, while for most liquids it is generally much more than 1 [35]. A high Prandtl number indicates almost adiabatic fluid. For $Pr \rightarrow \infty$, Eq. (17) shows that $\lambda_3 = 0$ while $\lambda_{4,5} = -\alpha_* \pm \sqrt{\alpha_*^2 - 1/\eta^2}$. Therefore, in this limit the entropic mode simply convects without diffusion while the diffusion of the acoustic modes for $\eta < \eta_b$ are independent of η and only depends on κ/μ

as also noted through Eq. (32).

The variation of the dispersion function $\widehat{\mathcal{M}}_5$ with depressed wavenumber η is for various values of Pr ranging from 0.5 to 1 is similar to what is shown in Fig. 6(c). For a given κ/μ , there is a definite value of Pr for which $(\eta_b)_{max}$ was noted. For a fixed κ/μ and γ , as Pr is varied, the variation of the relative diffusion characteristic ν_j/ν_1 either follows T_1 or T_2 as shown in Fig. 7(b) and 7(c), respectively. At lower κ/μ , trend T_1 is noted while for higher values of κ/μ trend T_2 is noted. Intermediate between the trends T_1 and T_2 , T_0 is noted at a particular value of $Pr = Pr_*$. The value of Pr_* is noted to decrease with κ/μ for a fixed γ . We have noted for $\gamma = 1.4$, $Pr_* = 0.75$ and 0.6316 for $\kappa/\mu = 0$ and 0.25 , respectively. These results are noted here for brevity.

3.8. Estimation of κ/μ for significant disturbance evolution

We have noted in Figs. 4 and 5 that, relatively significant disturbance evolution is noted for the case which are close to the parameters for which η_b is maximum. Following this principle, we next try to track the conditions for which η_b is maximum for variations in γ and Pr . This would give one idea regarding the range of parameters for which relatively significant disturbance (mostly acoustic) evolution may be noted in the physical plane. In Fig. 8(a,b), we plot η_b as a function of γ and Pr , respectively for indicated values of bulk viscosity ratio κ/μ . For Fig. 8(a), $Pr = 0.72$ while for Fig. 8(b), $\gamma = 1.4$ are used. One notes from Fig. 8(a) that except for the case $\kappa/\mu = 0$ where η_b monotonically decreases with γ , there exists a particular value of γ for which η_b is maximum. This value of γ is noted to increase with κ/μ . Similarly, for fixed γ and κ/μ , there is a definite value of Pr for which η_b is maximum. We note that this particular value of Pr for which η_b is maximum, decreases with increase in κ/μ .

It is to be noted that the discriminant for the cubic equation for η_b^2 i.e., Eq. (21) is negative. As discussed in Appendix-I, therefore, all the three roots are real (see Eq. (38)), while one of these are the real physical one. In fact, these three real roots are the x -coordinates of three points which lie on a circle in the complex plane with radius \hat{r} and center at $b/3$ as given by Eq. (38) in Appendix-I. In Fig. 8(c), we plot $\log(\hat{r})$ for the cubic Eq. (21) as a function of κ/μ and γ for $Pr = 0.72$. Here, γ is varied from 1 to 2, while κ/μ varies from 0 to 1. We note that $\log(\hat{r})$ is maximum along the line denoted by AB in Fig. 8(c). The empirical equation of this line may be given as $\kappa/\mu = 1.3705\gamma - 1.302$. This line denotes the value of κ/μ for which η_b is maximum for a given value of γ for $Pr = 0.72$. At $Pr = 0.72$ and $\gamma = 1.4$, $\kappa/\mu = 0.616$ for maximum η_b , which is almost same as that predicted by Fig. 2(c). Similarly, when we plot $\log(\hat{r})$ in the $(\kappa/\mu, 1/Pr)$ -plane for $\gamma = 1.4$ in Fig. 8(d), we see $\log(\hat{r})$ is maximum along the line CD whose equation is obtained as $\kappa/\mu = 1.382/Pr - 1.308$. In plotting Fig. 8(d), we choose $1/Pr$ as the ordinate as we note that the Prandtl number appears in the dispersion relationship as $1/Pr$ (see Sec. 5.4 in Appendix-I). From the above equation one finds that at $Pr = 0.72$ and $\gamma = 1.4$, $\kappa/\mu = 0.611$ for maximum η_b which is also close to the value predicted in Fig. 2(c). Combining these two equation, we suggest that for a given γ and Pr , the value of κ/μ for maximum η_b may be obtained empirically from

$$\frac{\kappa}{\mu} = 2.657 (1.3705\gamma - 1.302) \left(\frac{1.382}{Pr} - 1.308 \right) \quad (33)$$

The implication of the above equation is that for a given γ and Pr , one can predict the value of bulk viscosity ratio κ/μ close to which relatively significant acoustic disturbance evolution may be noted as also shown in Sec. 3.5. This of course needs to be verified from detailed investigations using direct numerical simulations.

4. Summary and conclusion

Here, the characteristics of the dispersion relation for 3D linearized compressible NSE is presented. The 3D compressible NSE supports five type of waves, two vortical, one entropic and two acoustic modes. The vortical modes are non-dispersive but diffusive in nature. The diffusion coefficient of the vortical mode is $\nu_{1,2} = -K^2/Re$ and therefore is independent of the Mach number. The entropic mode is also non-dispersive but diffusive in nature. In contrast, the acoustic modes are dispersive only up to a certain bifurcation wavenumber K_b . Beyond K_b relative diffusion of one acoustic mode increases while that for the other decreases with wavenumber. If the non-dimensional mean flow is denoted as $\mathbf{c} = (c_x, c_y, c_z)$, then the dispersion relation is given as $\omega_j = \beta - i\Lambda_j$. Here, we denote the vortical modes by $j = 1, 2$, the entropic mode by $j = 3$ and the two acoustic modes by $j = 4, 5$. The dispersion relation for the entropic and the acoustic modes are given by the cubic Eq. (16). From the analysis presented here, we conclude the following points as enumerated below.

1. The relative diffusion coefficient for entropic and acoustic modes $\nu_{3,4,5}/\nu_1$ and dispersion function for acoustic modes $\widehat{\mathcal{M}}_{4,5} = \Lambda_{jI}M^2/Re$ only depends upon the depressed wavenumber $\eta = KM/Re$, the bulk viscosity ratio κ/μ , specific heat ratio γ and Prandtl number Pr of the flow.
2. At lower wavenumber components, the deviation of the dispersion function from the inviscid and adiabatic case is proportional to η^2 at the leading order. The asymptotic expansion of the dispersion function and the relative diffusion coefficients of the entropic and acoustic modes for lower wavenumber components ($\eta < 1$) is given in Sec. 3.2. For long wavelength disturbances, the relative diffusion coefficients of the entropic and acoustic modes increase linearly with κ/μ and γ while varying inversely with Pr .
3. When the bulk viscosity ratio is increased, the shape and extent of the dispersion function is altered significantly as described in Sec. 3.3. The change is more significant for higher wavenumber components. We note that the depressed bifurcation wavenumber $\eta_b = K_bM/Re$ is maximum when $\kappa/\mu \simeq 0.6$ for $\gamma = 1.4$ and $Pr = 0.72$. Similar critical values of γ and Pr are also noted to exist for which η_b is maximum.
4. The relative diffusion coefficient for entropic and acoustic modes displays three types of trends depending upon κ/μ , γ and Pr , denoted here as T_0 , T_1 and T_2 . Following the trend T_0 , the relative diffusion

coefficients are independent of wavenumber. The trend T_1 corresponds to the case when ν_3/ν_1 monotonically increases while $\nu_{4,5}/\nu_1$ for $\eta < \eta_b$ monotonically decreases with η . The reverse scenario is noted for the trend T_2 .

5. The smallest wavelength of the acoustic dispersive disturbances are noted to be of the similar order or one order higher than the mean-free path for most common dilute gases.
6. Lastly, we have empirically obtained a criterion on the bulk viscosity ratio κ/μ depending upon γ and Pr for which η_b would be maximum. The significance of this criterion is that relatively significant evolution of acoustic and/or entropic disturbances are noted when the κ/μ is close to this critical value. This is established here considering linearized disturbance evolution for a given initial condition composed of entropic and acoustic disturbances as illustrated in Sec. 3.5. The last aspect needs to be further verified from detailed investigations using direct numerical simulations.

References

- [1] L. D. Landau, E. M. Lifshitz, Course of theoretical physics, Elsevier, 2013.
- [2] G. B. Whitham, Linear and nonlinear waves, Vol. 42, John Wiley & Sons, 2011.
- [3] J. Lighthill, Waves in fluids, Cambridge university press, 2001.
- [4] L. D. Landau, E. M. Lifšic, E. M. Lifshitz, A. M. Kosevich, L. P. Pitaevskii, Theory of elasticity: volume 7, Vol. 7, Elsevier, 1986.
- [5] T. Colonius, S. K. Lele, P. Moin, Sound generation in a mixing layer, *Journal of Fluid Mechanics* 330 (1997) 375–409.
- [6] C. K. Tam, Recent advances in computational aeroacoustics, *Fluid dynamics research* 38 (9) (2006) 591.
- [7] S. Moreau, The third golden age of aeroacoustics, *Physics of Fluids* 34 (3) (2022) 031301.
- [8] S. K. Lele, J. W. Nichols, A second golden age of aeroacoustics?, *Philosophical Transactions of the Royal Society A: Mathematical, Physical and Engineering Sciences* 372 (2022) (2014) 20130321.
- [9] C. Bailly, C. Bogey, O. Marsden, Progress in direct noise computation, *International Journal of Aeroacoustics* 9 (1-2) (2010) 123–143.
- [10] S. Unnikrishnan, D. V. Gaitonde, Transfer mechanisms from stochastic turbulence to organized acoustic radiation in a supersonic jet, *European Journal of Mechanics-B/Fluids* 72 (2018) 38–56.
- [11] D. González, R. Speth, D. Gaitonde, M. Lewis, Finite-time lyapunov exponent-based analysis for compressible flows, *Chaos: An Interdisciplinary Journal of Nonlinear Science* 26 (8) (2016) 083112.

- [12] R. E. Graves, B. M. Argrow, Bulk viscosity: past to present, *Journal of Thermophysics and Heat Transfer* 13 (3) (1999) 337–342.
- [13] B. Sharma, R. Kumar, S. Pareek, Bulk viscosity of dilute gases and their mixtures, *Fluids* 8 (1) (2023) 28.
- [14] P. K. Kundu, I. M. Cohen, D. R. Dowling, *Fluid Mechanics*, Academic press, 2015.
- [15] P. Ramond, The Abel–Ruffini Theorem: Complex but Not Complicated, *The American Mathematical Monthly* 129 (3) (2022) 231–245.
- [16] S. Ansumali, I. V. Karlin, H. C. Öttinger, Thermodynamic theory of incompressible hydrodynamics, *Physical review letters* 94 (8) (2005) 080602.
- [17] A. Sommerfeld, *Thermodynamics and statistical mechanics*, Vol. 5, CUP Archive, 1964.
- [18] E. W. Weisstein, Cubic formula, <https://mathworld.wolfram.com/>.
- [19] S. Benjelloun, J.-M. Ghidaglia, On the dispersion relation for compressible Navier-Stokes Equations, arXiv preprint arXiv:2011.06394.
- [20] I. Karlin, Derivation of regularized Grad’s moment system from kinetic equations: modes, ghosts and non-Markov fluxes, *Philosophical Transactions of the Royal Society A: Mathematical, Physical and Engineering Sciences* 376 (2118) (2018) 20170230.
- [21] C. Frouzakis, S. Ansumali, I. Karlin, I. Kevrekidis, Entropic Lattice Boltzmann Study of Hydrodynamics in a Micro cavity, Under consideration for publication in *Journal of Fluid Mechanics*.
- [22] H. Struchtrup, M. Torrilhon, Regularization of grad’s 13 moment equations: Derivation and linear analysis, *Physics of Fluids* 15 (9) (2003) 2668–2680.
- [23] H. Okumura, F. Yonezawa, New formula for the bulk viscosity constructed from the interatomic potential and the pair distribution function, *The Journal of Chemical Physics* 116 (17) (2002) 7400–7410.
- [24] M. S. Cramer, Numerical estimates for the bulk viscosity of ideal gases, *Physics of fluids* 24 (6) (2012) 066102.
- [25] F. Jaeger, O. K. Matar, E. A. Müller, Bulk viscosity of molecular fluids, *The Journal of chemical physics* 148 (17) (2018) 174504.
- [26] J. Shang, T. Wu, H. Wang, C. Yang, C. Ye, R. Hu, J. Tao, X. He, Measurement of temperature-dependent bulk viscosities of Nitrogen, Oxygen and Air from spontaneous Rayleigh-Brillouin scattering, *IEEE Access* 7 (2019) 136439–136451.

- [27] S. Pirozzoli, T. Colonius, Generalized characteristic relaxation boundary conditions for unsteady compressible flow simulations, *Journal of Computational Physics* 248 (2013) 109–126.
- [28] P. Doak, Momentum potential theory of energy flux carried by momentum fluctuations, *Journal of sound and vibration* 131 (1) (1989) 67–90.
- [29] D. Cai, D. W. McLaughlin, K. T. McLaughlin, The nonlinear Schrödinger equation as both a PDE and a dynamical system, *Handbook of dynamical systems* 2 (2002) 599–675.
- [30] S. Jennings, The mean free path in air, *Journal of Aerosol Science* 19 (2) (1988) 159–166.
- [31] F. M. White, *Fluid mechanics*, 1966.
- [32] G. Karniadakis, A. Beskok, N. Aluru, *Microflows and nanoflows: fundamentals and simulation*, Vol. 29, Springer Science & Business Media, 2006.
- [33] S. B. Pope, *Turbulent flows*, Cambridge university press, 2000.
- [34] J. Hilsenrath, C. W. Beckett, W. S. Benedict, L. Fano, H. J. Hoge, J. F. Masi, R. L. Nuttall, Y. S. Touloukian, H. W. Woolley, *Tables of thermal properties of gases: comprising tables of thermodynamic and transport properties of Air, Argon, Carbon dioxide, Carbon monoxide, Hydrogen, Nitrogen, Oxygen, and Steam*, Vol. 564, US Department of Commerce, National Bureau of Standards, 1955.
- [35] D. J. Tritton, *Physical fluid dynamics*, Springer Science & Business Media, 2012.

5. Appendix-I

Here, the general solution solution of a cubic polynomial equation with real coefficients as given below is considered for the ease of the reader. Such equations can be symbolically written as

$$x^3 + bx^2 + cx + d = 0 \quad (34)$$

Following the substitution $y = (x - b/3)$ in the above equation, one gets the depressed cubic equation

$$y^3 + py + q = 0 \quad (35)$$

where,

$$p = \left(c - \frac{b^2}{3} \right) \quad \text{and} \quad q = \left(\frac{2}{27}b^3 - \frac{1}{3}bc + d \right)$$

Following Vieta's substitution [18] $y = (w - \frac{p}{3w})$ to Eq. (35), one obtains

$$w^3 - \frac{p^3}{27w^3} + q = 0 \quad (36)$$

Equation (36) is in essence a quadratic equation, which can be solved to obtain the solution for w^3 as

$$w^3 = \left[-\frac{q}{2} \pm \sqrt{\Delta} \right]$$

where, the discriminant Δ is given as

$$\Delta = \left(\frac{p^3}{27} + \frac{q^2}{4} \right) \quad (37)$$

Depending upon whether Δ is positive or negative or equal to zero, one obtains three different classes of the solution.

5.1. Solution for $\Delta < 0$

As $\Delta < 0$, one notes that $\Delta = -a^2$ where a is a real positive number. Moreover, from Eq. (37) for this case one also notes that $p < -s$, where $s = \sqrt[3]{(27q^2/4)} > 0$. Let, R_1 and R_2 represent the two solutions of the Eq. (37) such that $R_1 = \left((-q/2) + \sqrt{\Delta} \right) = Re^{i\psi}$ and $R_2 = \left((-q/2) - \sqrt{\Delta} \right) = Re^{-i\psi}$ where, $R = \sqrt{(-q/2) + a^2}$ and $\psi = \tan^{-1}(-2a/q)$. The general solution of the cubic equation Eq. (34) for this case is given as

$$x_{1,2,3} = \frac{b}{3} + \begin{cases} 2\hat{r} \cos\left(\frac{\psi}{3}\right) \\ 2\hat{r} \cos\left(\frac{\psi}{3} + \frac{2\pi}{3}\right) \\ 2\hat{r} \cos\left(\frac{\psi}{3} - \frac{2\pi}{3}\right) \end{cases} \quad (38)$$

where $\hat{r} = \sqrt{-p/3}$. Here, all the three solutions are real.

5.2. Solution for $\Delta > 0$

As $\Delta > 0$, both R_1 and R_2 are real numbers. The general solution of the cubic equation Eq. (34) for this case is given as

$$x_{1,2,3} = \frac{b}{3} + \begin{cases} u_1 \\ -\frac{1}{2}u_1 + i\frac{\sqrt{3}}{2}v_1 \\ -\frac{1}{2}u_1 - i\frac{\sqrt{3}}{2}v_1 \end{cases} \quad (39)$$

where $u_1 = (\sqrt[3]{R_1} + \sqrt[3]{R_2})$ and $v_1 = (\sqrt[3]{R_1} - \sqrt[3]{R_2})$. For this case, x_1 is real while x_2 and x_3 are complex conjugates.

5.3. Solution for $\Delta = 0$

As $\Delta > 0$, here $R_1 = R_2 = (-q/2)$ and hence, the general solution of the cubic equation Eq. (34) for this case is given as

$$x_{1,2,3} = \frac{b}{3} + \begin{cases} 2\sqrt[3]{(-q/2)} \\ -\sqrt[3]{(-q/2)} \\ -\sqrt[3]{(-q/2)} \end{cases} \quad (40)$$

Here, all the roots are real with two identical roots corresponding to x_2 and x_3 .

5.4. Connection with the cubic dispersion equation

The cubic polynomial dispersion equation for the entropic and the two acoustic modes are given by Eq. (17). Comparing Eq. (17) with Eq. (34), one gets $b = C_8$, $c = (C_5 + 1/\eta^2)$ and $d = C_7/\eta^2$. From the general solution of the cubic polynomial equation we note the existence of three important parameters, *viz.* $(-p/3)$, $(-q/2)$ and the discriminant $\Delta = (p^3/27 + q^2/4)$, which in terms of η are given as

$$(-p/3) = a_0 - \frac{1}{3} \left(\frac{1}{\eta^2} \right) \quad (41)$$

$$(-q/2) = b_0 + b_1 \left(\frac{1}{\eta^2} \right) \quad (42)$$

$$\Delta = d_0 + d_1 \left(\frac{1}{\eta^2} \right) + d_2 \left(\frac{1}{\eta^4} \right) + \frac{1}{27} \left(\frac{1}{\eta^6} \right) \quad (43)$$

where the above coefficients as functions of κ/μ , γ and Pr are given as

$$\begin{aligned} a_0 &= \left(\frac{1}{9} \right) \left(\frac{\kappa}{\mu} \right)^2 + \left(\frac{8}{27} \right) \left(\frac{\kappa}{\mu} \right) - \left(\frac{1}{9} \right) \left(\frac{\gamma}{Pr} \right) \left(\frac{\kappa}{\mu} \right) - \left(\frac{4}{27} \right) \left(\frac{\gamma}{Pr} \right) + \left(\frac{1}{9} \right) \left(\frac{\gamma}{Pr} \right)^2 + \left(\frac{16}{81} \right) \\ b_0 &= - \left(\frac{16}{81} \right) \left(\frac{\kappa}{\mu} \right) - \left(\frac{4}{27} \right) \left(\frac{\kappa}{\mu} \right)^2 - \left(\frac{1}{27} \right) \left(\frac{\kappa}{\mu} \right)^3 + \left(\frac{8}{81} \right) \left(\frac{\gamma}{Pr} \right) + \left(\frac{2}{27} \right) \left(\frac{\gamma}{Pr} \right)^2 \\ &\quad - \left(\frac{1}{27} \right) \left(\frac{\gamma}{Pr} \right)^3 + \left(\frac{1}{18} \right) \left(\frac{\gamma}{Pr} \right) \left(\frac{\kappa}{\mu} \right)^2 + \left(\frac{1}{18} \right) \left(\frac{\gamma}{Pr} \right)^2 \left(\frac{\kappa}{\mu} \right) + \left(\frac{4}{27} \right) \left(\frac{\gamma}{Pr} \right) \left(\frac{\kappa}{\mu} \right) - \left(\frac{64}{729} \right) \\ b_1 &= \left(\frac{2}{9} \right) + \left(\frac{1}{6} \right) \left(\frac{\kappa}{\mu} \right) - \left(\frac{1}{2} \right) \left(\frac{1}{Pr} \right) + \left(\frac{1}{6} \right) \left(\frac{\gamma}{Pr} \right) \\ d_0 &= - \left(\frac{64}{2187} \right) \left(\frac{\gamma}{Pr} \right)^2 + \left(\frac{32}{729} \right) \left(\frac{\gamma}{Pr} \right)^3 - \left(\frac{4}{243} \right) \left(\frac{\gamma}{Pr} \right)^4 - \left(\frac{64}{729} \right) \left(\frac{\gamma}{Pr} \right)^2 \left(\frac{\kappa}{\mu} \right) \\ &\quad + \left(\frac{8}{81} \right) \left(\frac{\gamma}{Pr} \right)^3 \left(\frac{\kappa}{\mu} \right) - \left(\frac{2}{81} \right) \left(\frac{\gamma}{Pr} \right)^4 \left(\frac{\kappa}{\mu} \right) - \left(\frac{8}{81} \right) \left(\frac{\gamma}{Pr} \right)^2 \left(\frac{\kappa}{\mu} \right)^2 - \left(\frac{4}{81} \right) \left(\frac{\gamma}{Pr} \right)^2 \left(\frac{\kappa}{\mu} \right)^3 \\ &\quad - \left(\frac{1}{108} \right) \left(\frac{\gamma}{Pr} \right)^2 \left(\frac{\kappa}{\mu} \right)^4 + \left(\frac{2}{27} \right) \left(\frac{\gamma}{Pr} \right)^3 \left(\frac{\kappa}{\mu} \right)^2 + \left(\frac{1}{54} \right) \left(\frac{\gamma}{Pr} \right)^3 \left(\frac{\kappa}{\mu} \right)^3 - \left(\frac{1}{108} \right) \left(\frac{\gamma}{Pr} \right)^4 \left(\frac{\kappa}{\mu} \right)^2 \\ d_1 &= + \left(\frac{1}{27} \right) \left(\frac{1}{Pr} \right) \left(\frac{\kappa}{\mu} \right)^3 - \left(\frac{1}{54} \right) \left(\frac{\gamma}{Pr} \right) \left(\frac{\kappa}{\mu} \right)^3 + \left(\frac{2}{27} \right) \left(\frac{\gamma}{Pr} \right)^2 \left(\frac{\kappa}{\mu} \right)^2 \\ &\quad - \left(\frac{1}{18} \right) \left(\frac{\gamma}{Pr} \right) \left(\frac{1}{Pr} \right) \left(\frac{\kappa}{\mu} \right)^2 - \left(\frac{2}{27} \right) \left(\frac{\gamma}{Pr} \right) \left(\frac{\kappa}{\mu} \right)^2 + \left(\frac{4}{27} \right) \left(\frac{1}{Pr} \right) \left(\frac{\kappa}{\mu} \right)^2 \\ &\quad + \left(\frac{16}{81} \right) \left(\frac{1}{Pr} \right) \left(\frac{\kappa}{\mu} \right) - \left(\frac{8}{81} \right) \left(\frac{\gamma}{Pr} \right) \left(\frac{\kappa}{\mu} \right) - \left(\frac{4}{27} \right) \left(\frac{\gamma}{Pr} \right) \left(\frac{1}{Pr} \right) \left(\frac{\kappa}{\mu} \right) \\ &\quad + \left(\frac{16}{81} \right) \left(\frac{\gamma}{Pr} \right)^2 \left(\frac{\kappa}{\mu} \right) - \left(\frac{1}{18} \right) \left(\frac{\gamma}{Pr} \right)^2 \left(\frac{1}{Pr} \right) \left(\frac{\kappa}{\mu} \right) - \left(\frac{1}{54} \right) \left(\frac{\gamma}{Pr} \right)^3 \left(\frac{\kappa}{\mu} \right) \\ &\quad + \left(\frac{64}{729} \right) \left(\frac{1}{Pr} \right) - \left(\frac{32}{729} \right) \left(\frac{\gamma}{Pr} \right) + \left(\frac{32}{243} \right) \left(\frac{\gamma}{Pr} \right)^2 - \left(\frac{8}{81} \right) \left(\frac{\gamma}{Pr} \right) \left(\frac{1}{Pr} \right) \\ &\quad - \left(\frac{2}{27} \right) \left(\frac{\gamma}{Pr} \right)^2 \left(\frac{1}{Pr} \right) - \left(\frac{2}{81} \right) \left(\frac{\gamma}{Pr} \right)^3 + \left(\frac{1}{27} \right) \left(\frac{\gamma}{Pr} \right)^3 \left(\frac{1}{Pr} \right) \\ d_2 &= - \left(\frac{1}{108} \right) \left(\frac{\kappa}{\mu} \right)^2 - \left(\frac{2}{81} \right) \left(\frac{\kappa}{\mu} \right) - \left(\frac{1}{6} \right) \left(\frac{1}{Pr} \right) \left(\frac{\kappa}{\mu} \right) + \left(\frac{5}{54} \right) \left(\frac{\gamma}{Pr} \right) \left(\frac{\kappa}{\mu} \right) \\ &\quad + \left(\frac{1}{4} \right) \left(\frac{1}{Pr} \right)^2 - \left(\frac{1}{6} \right) \left(\frac{\gamma}{Pr} \right) \left(\frac{1}{Pr} \right) - \left(\frac{1}{108} \right) \left(\frac{\gamma}{Pr} \right)^2 - \left(\frac{2}{9} \right) \left(\frac{1}{Pr} \right) \\ &\quad + \left(\frac{10}{81} \right) \left(\frac{\gamma}{Pr} \right) - \left(\frac{4}{243} \right) \end{aligned}$$